

**A CYLINDRICAL FREQUENCY SELECTIVE
SURFACE COMPRISING OF METAL STRIPS**

77704

A MASTER'S THESIS

in

77704

Electrical and Electronics Engineering

University of Gaziantep

By

Ali UZER

December, 1998

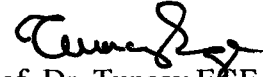
Approval of the Graduate School of Natural and Applied Sciences



Assoc. Prof. Dr. Ali Rıza TEKİN

Director

I certify that this thesis satisfies all the requirements as a thesis for the degree of Master of Science.



Prof. Dr. Tuncay EGE

Chairman of the Department


I certify that I have read this thesis and that in my opinion it is fully adequate, in scope and quality, as a thesis for the degree of Master of Science.




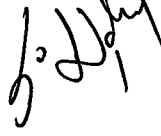
Prof. Dr. Tuncay EGE

Supervisor

Examining Committee in Charge:

Prof. Dr. Saadettin ÖZYAZICI (Chairman) 

Prof. Dr. Tuncay EGE 

Asst. Prof. Dr. Savaş UÇKUN 

ABSTRACT

A CYLINDRICAL FREQUENCY SELECTIVE SURFACE COMPRISING OF METAL STRIPS

UZER Ali

M.S. in Electrical and Electronics Engineering

Supervisor: Prof. Dr. Tuncay EGE

December 1998, 63 Pages

In this study, a circular cylindrical structure covered periodically with freestanding metal strips are considered as a frequency selective surface. Floquet's theorem, which inherently takes all mutual couplings between elements into account, is utilized in the formulation of the problem. Formulations are presented for calculating induced currents over the strips first and later the transmission and reflection coefficients are expressed in terms of those induced currents. Plots are given for some representative values of surface periodicities and the results are compared with some planar frequency selective surface results. As in the study of previous works on planar frequency selective surfaces, a bandpass response is also found in our cylindrical frequency selective surface and the similarities are stated.

Keywords: FSS, Dicroic surfaces, Cylindrical Floquet Modes.

ÖZET

METAL ŞERİTLERDEN OLUŞMUŞ SİLİNDİRİK FREKANS SEÇİCİ YÜZEY

UZER, Ali

Yüksek Lisans Tezi, Elektrik ve Elektronik Mühendisliği Bölümü

Tez Yöneticisi: Prof. Dr. Tuncay EGE

Aralık 1998, 63 sayfa

Bu çalışmamızda silindirik bir yüzey üzerine yerleştirilmiş olan metal şeritler bir frekans seçici yüzey olarak ele alındı ve incelendi. Floquet teoremi kullanılarak indüs olan akımlarla ilgili formüller yazıldı, daha sonra yüzeyden geçme ve yansıma katsayıları bu akımlar cinsinden ifade edildi. Son olarak da bazı yüzey değerleri için yansıma ve geçme katsayıları hesaplandı ve frekansa göre çizildi. Ayrıca sonuçlar düzlemsel frekans seçici yüzeylerle karşılaştırıldı ve benzerlikler ifade edildi.

Anahtar Kelimeler: Frekans Seçici Yüzeyler, Eğimli Yüzeyler, Silindirik Floquet Modlar

ACKNOWLEDGEMENT

I would like to express my sincerest gratitude to the perfect teacher and supervisor Prof. Dr. Tuncay Ege for his guidance, suggestions, valuable criticism and great help in preparation of the theory and some mathematical softwares for numerical analysis.



TABLE OF CONTENTS

	Page
ABSTRACT.....	iii
ÖZET.....	iv
ACKNOWLEDGEMENT.....	v
TABLE OF CONTENTS.....	vi
LIST OF FIGURES.....	viii
1. INTRODUCTION.....	1
2. PERIODIC STRUCTURES AND FLOQUET'S MODES.....	6
2.1. Periodic Excitation of a Periodic Planar Structure.....	6
2.2. Periodic Excitation of a Periodic Cylindrical Structure.....	8
3. A TWO DIMENSIONAL DIPOLE ARRAY ON A CYLINDRICAL STRUCTURE.....	11
3.1. Array Model.....	12
3.2. Active Dipole Current.....	13
3.3. Method Of Moments.....	18
3.4. Active Gap Impedance.....	21
3.5. Active Array Fields.....	22

3.6. Numerical Analysis.....	24
4. A CYLINDRICAL FREQUENCY SELECTIVE SURFACE.....	27
4.1. Passive Array Currents.....	28
4.2. Moment Method Matrix Equation.....	32
4.3. Reflection And Transmission Coefficients.....	36
5. NUMERICAL RESULTS.....	41
5.1. Some Representative Calculations.....	41
5.2. Comparison With Other Results.....	48
6. CONCLUSION.....	51
REFERENCES.....	53
APPENDIX A FIELDS OF A PHASED LINE SOURCE.....	55
APPENDIX B CONVERGENCE ACCELERATION FOR THE MATRIX ELEMENTS.....	59

LIST OF FIGURES

Figure	Page
1.1. A frequency selective surface as a subreflector.....	2
2.1. A periodic planar structure excited by an incident field on x-y plane.....	6
2.2. A periodic cylindrical surface.....	9
3.1. Geometry of the problem.....	11
3.2. Unit cell geometry.....	25
3.3. Voltage element gain pattern of an axial dipole in a periodic cylindrical array. Parameter: elevation angle $\theta = 90,60,30$	26
4.1. A cylindrical surface covered periodically with metal strips.....	27
5.1. Unit cell geometry.....	41
5.2. Frequency versus TM reflection and transmission coefficients. Parameter: width of the strip W.....	44
5.3. Frequency versus TM reflection and transmission coefficients. Parameter: length of the strip L.	44
5.4. Frequency versus TM reflection and transmission coefficients. Parameter: length of the unit cell D.	45
5.5. Frequency versus TM reflection and transmission coefficients. Parameter: width of the unit cell B.....	45

5.6. Frequency versus TM reflection and transmission coefficients. Parameter: number of strips in a ring N	46
5.7. Frequency versus TM reflection and transmission coefficients. Parameter: angle of incidence θ	46
5.8. Frequency versus TM reflection and transmission coefficients for the incidence angle $\theta = 60$. Parameter: length of the strip L	47
5.9. Comparison to planar FSS given in [9].....	50
5.10. Comparison to planar FSS given in [10].....	50



CHAPTER 1

INTRODUCTION

Measurements has demonstrated that a periodic surface has bandpass and bandstop characteristics when illuminated by an incident electromagnetic wave of variable frequency. There are many important structures whose characteristics are periodic in space. Examples are three-dimensional lattice structures for crystals, artificial dielectrics consisting of periodically placed conducting pieces, and waveguides with periodic loadings. Waves along these structures exhibit a unique frequency dependence often characterized by stopbands and passbands This property makes these structures useful for many applications.

Basically an FSS can be of two types, either in the form of a periodically perforated screens (apertures), or in the form of an array of metallic patches printed on a dielectric support structure. At a specific frequency, the surface exhibit a total transmission for the screen case, or a total reflection for the patch element case. Such a specific frequency is called as the resonance frequency and it depends both on the shape of the single element (patch/slot) and on the mutual coupling which arises from nearby elements in the array. Also by cascading several stages, or placing various self-resonating grids at close distance, one should obtain wider operation bandwidth and sharper cut-off, as it has been shown by several authors [12-15].

1.1. Typical Applications

The typical applications of frequency selective surfaces (FSS) are many and varied, and they range over much of the electromagnetic spectrum. In the microwave region, the frequency selective properties of periodic screens are exploited, for example, to make more efficient use of reflector antennas. As shown in Figure 1.1., a frequency selective surface can be placed between two feeds, radiating at different frequencies. Then the resonance frequency of the surface may be adjusted such that the surface becomes totally reflective over the operating band of feed 1, and conversely it becomes nearly transparent over the operating band of feed 2. Hence, by this configuration, two independent feeds may share the same reflector antenna simultaneously [11].

A next example of the exploitation of the frequency selective property of periodic screens in the microwave region is the application in radome design [11]. The screen can be tuned to provide a bandpass transmission characteristic at the operating frequency of the antenna. At the out-of-band frequencies, the screen can be made totally reflecting, and the radome can be designed to blend with the skin of the vehicle such that minimal scattering occurs at the joint between the radome and the skin.

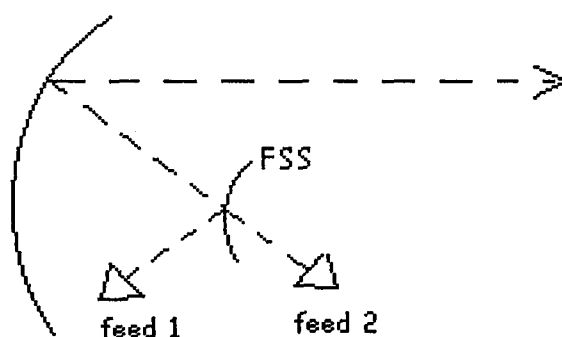


Figure 1.1. A frequency selective surface as a subreflector

In the far-infrared region, periodic screens are used as polarizers, beam splitters, as well as mirrors for improving the pumping efficiency in molecular lasers

[11]. A polarizer can be constructed from a diffraction grating such that the fields polarized parallel to the grating are reflected, while those with an orthogonal polarization are transmitted. A cavity mirror used in a laser can be constructed from a frequency selective surface such that it is totally reflecting at the wavelength of the energy used to pump the cavity, and partially transmitting (0-40 percent) at the lasing wavelength. By the way, the efficiency of the system is increased.

Another application of the FSS in the far-infrared region is infrared sensors where the frequency selective property of the FSS is used to absorb the desired frequencies in the substrate material backing the screen, while the out-of-band frequencies are rejected [11].

In the near-infrared and visible portions of the spectrum, periodic screens have been proposed as solar selective surfaces to aid in the collection of solar energy [11]. A screen can be designed such that it is essentially transparent in the frequency band where the solar cells are most efficient and is reflecting at frequencies outside this band.

1.2. Previous Works

Various approaches have been used to predict the scattering from frequency selective surfaces. The problem of scattering by a two dimensional periodic array of rectangular plates was investigated by Ott, Kouyoumjian, and Peters [16]. The solution given is restricted to the case of narrow plates arranged in a rectangular lattice with a normally incident plane wave. The complementary problem of scattering by a conducting screen perforated periodically with apertures was analyzed by Keiburtz and Ishimaru [17] by the variational method.

In 1970, a more general formulation to the scattering problem for two dimensional periodic array of plates was presented by C. C. Chen [10]. The field distribution was expanded into a set of Floquet mode functions, and an integral equation was obtained. Then he had determined the unknown induced current by using the method of moments.

In 1975, J. P. Montgomery [18] gave the solutions to the unsymmetrical problems of scattering of a plane wave by an infinite periodic array of thin conductors.

Later, Tsao and Mittra [19] in 1982, presented an iterative procedure in spectral domain to solve simultaneously for the current distribution and the aperture field of an FSS. They derived a differential equation, based on the Floquet mode expansion and the electromagnetic boundary conditions. They also presented a full wave analysis of both the cross shaped and Jerusalem type elements.

In the area of two dimensional cylindrical or spherical frequency selective surfaces no previous work can be found in the literature but Cwick [2] has explained a general procedure for analyzing such surfaces. He also applied his methods to a cylindrical surface of periodically placed infinite strips, but that was a one dimensional problem. Although many practical frequency selective surfaces such as the hyperbolic subreflector and the spherical radomes are curved, an infinite planar model is often used to analyze these surfaces approximately because their exact analysis is intractable except for a cylindrical or spherical geometry [2].

1.3. Methods of This Work

When analyzing a general periodic surface with the modal approach, one begins by reducing the formulation which holds for the infinite periodic surface to one which holds over a single periodic cell. This is accomplished by recognizing that a periodic excitation produces a periodic response. Hence, the scattered fields from the surface may be represented by a superposition of periodic functions-the Floquet harmonics [11]. For a planarly periodic surface the Floquet harmonics are plane waves with propagation constants related to the surface periodicity and the incident field.

Similar to the planar case, an analysis that exploits the periodicity of the fields scattered or radiated from a periodic cylindrical surface requires a solution of Maxwell's equations in the cylindrical coordinate system. As in the planar surface,

the scattered fields can be represented by a superposition of Floquet harmonics. For a periodic cylindrical surface, analogous to the planar case, the Floquet harmonics are cylindrical waves with propagation constants related to the surface periodicity and the incident field [2]. In this work we have followed those procedures of Cwick [2] for the formulation of the problem.

In the Chapter 2 we give an introduction to Floquet's theorem and Floquet modes, for both planarly periodic and cylindrically periodic structures. Chapter 3 deals with a previous work on a phased array antenna problem whereby the Floquet theorem is used. At the end of Chapter 3, active array gap impedances and the element pattern of an axial dipole in a match terminated environment are evaluated to test the accuracy of the results with [3] and [4].

We give the main formulations of our work in the Chapter 4, in which, a cylindrically periodic structure covered with metal strips is considered as a frequency selective surface. Firstly the scattered fields on either side of the strips are expanded as a series of Floquet modes. Then they are related to the induced surface current density, through the standard electromagnetic boundary conditions. As a result an integral equation is obtained. That integral equation is solved for the induced current density by applying the method of moments, and later, the power reflection and transmission coefficients are expressed in terms of that induced current density.

The numerical results and discussions on the surface reflection and transmission coefficients, for some specific array geometries, are given in Chapter 5. Finally, Chapter 6 concludes on the results and the surface performance.

CHAPTER 2

PERIODIC STRUCTURES

AND FLOQUET'S MODES

2.1. Periodic Excitation of a Periodic Planar Structure

Before giving the Floquet modes of a cylindrically periodic surface it would be better to have a look on the Floquet modes of a planar surface. These modes have been extensively used in many frequency selective surface problems as well as the phased array antenna problems.

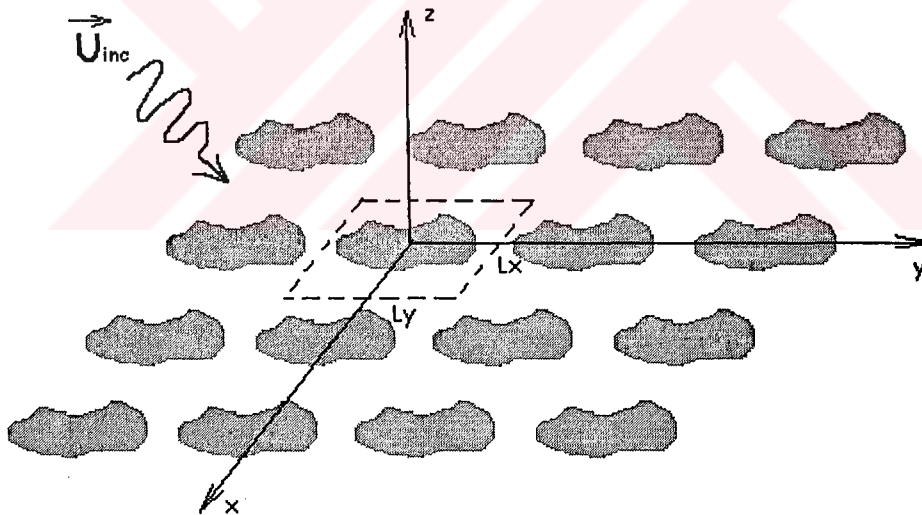


Fig. 2.1. A periodic planar structure excited by an incident field on x-y plane

For a periodic excitation, as shown in the Figure 2.1, the fields scattered from the periodic planar surface may be expressed in terms of the Floquet modes. But the periodicity of the excitation should be such that the magnitude remains constant and the phase changes linearly across the surface. On the other hand, an

arbitrary exciting field can be written as a sum of such periodic excitations [1]. Therefore without loss of generality, we can assume a periodic excitation U_i to the periodic planar surface as

$$U_i = A_i e^{-jk_x x} e^{-jk_y y} \quad (2.1)$$

with k_x and k_y representing linear phase variations along x and y directions respectively. Here U_i may be a TM, or TE wave. Now the response field U_r can be written in a series of space harmonics [1] such that

$$U_r = \sum_{m=-\infty}^{\infty} \sum_{n=-\infty}^{\infty} B_{mn} e^{-jk_{xm} x} e^{-jk_{yn} y} \quad (2.2)$$

where

$$k_{xm} = k_x + \frac{2\pi m}{L_x} \quad \text{and} \quad k_{yn} = k_y + \frac{2\pi n}{L_y}, \quad m, n = 0, \pm 1, \pm 2, \dots$$

This representation is also an extension of a one dimensional case[1]. Here L_x and L_y are surface periodicities in x and y directions respectively.

Note that, for the source free region, the scattered wave U_r satisfies the wave equation

$$(\nabla^2 + k_0^2)U_r(x, y, z) = 0$$

and it is separable with respect to x, y, and z. Then $k_0^2 = k_{xm}^2 + k_{yn}^2 + k_z^2$ and, for an arbitrary point in free space,

$$U_r(x, y, z) = \sum_{m=-\infty}^{\infty} \sum_{n=-\infty}^{\infty} B_{mn} \exp\left[-jk_{xm} x - jk_{yn} y - j(k^2 - k_{xm}^2 - k_{yn}^2)^{1/2} z\right] \quad (2.3)$$

The determination of the unknown complex coefficients B_{mn} can be made by applying the boundary conditions of the problem. Let us note that the propagation constant of (2.3) in z-direction $\beta_{mn} = (k_0^2 - k_{xm}^2 - k_{yn}^2)^{1/2}$ can be real or purely

imaginary depending on the linear phase variations of the incident field k_x, k_y and the integers m, n . If β_{mn} is real, the wave propagates away from the surface carrying real power and is called a grating mode. If β_{mn} is purely imaginary, the wave does not carry real power away from the surface and is called an evanescent mode [1].

Equation (2.3) can be written in the following symbolic form as

$$U_r(x, y, z) = \sum_{m=-\infty}^{\infty} \sum_{n=-\infty}^{\infty} B_{mn} \psi_{mn} e^{-j\beta_{mn}z} \quad (2.4.a)$$

where

$$\psi_{mn} = \frac{e^{-jk_{xm}x} e^{-jk_{yn}y}}{\sqrt{L_x L_y}}, \quad \beta_{mn}^2 = k^2 - k_{xm}^2 - k_{yn}^2 \quad (2.4.b)$$

One can easily show that, with respect to the inner product defined by

$$\langle f, g^* \rangle = \int_{-L_y/2}^{L_y/2} \int_{-L_x/2}^{L_x/2} f g^* dx dy \quad (2.5)$$

all Floquet modes ψ_{mn} are orthonormal to each other. These modes are the Floquet modes of the problem and each Floquet mode ψ_{mn} is associated with a propagation constant β_{mn} as given in (2.4.b)

2.2. Periodic Excitation of a Periodic Cylindrical Structure

The geometry of a surface periodic in the cylindrical coordinate system is shown in the Figure 2.2. The surface has the periodicities d in z -direction and α in ϕ -direction. The phase of the exciting field is allowed to vary linearly across the doubly periodic surface as

$$e^{-j\nu_0\phi} e^{-jk_{z0}z} \quad (2.6)$$

where k_{z0} is a real number and ν_0 is an integer due to the natural 2π periodicity

with respect to ϕ . The resultant Floquet modes, as given by Cwick [2], are

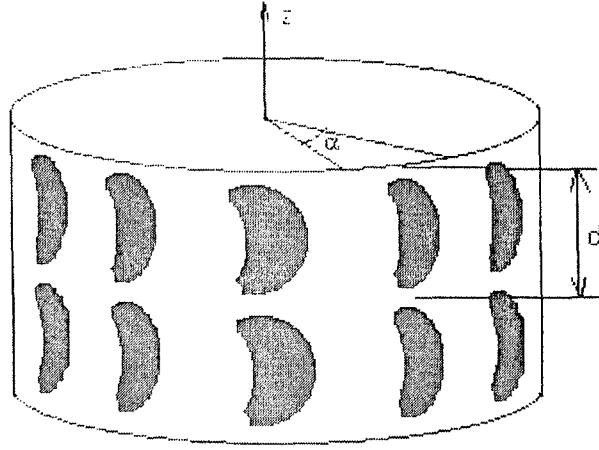


Fig. 2.2. A periodic cylindrical surface

$$\Psi_{mn} = \frac{e^{-jv_m\phi} e^{-jk_{zn}z}}{\sqrt{\alpha d}} \quad (2.7)$$

where

$$v_m = v_0 + \frac{2\pi m}{\alpha}, \quad k_{zn} = k_{z0} + \frac{2\pi n}{d} \quad m, n = 0, \pm 1, \pm 2, \pm 3, \dots$$

For the internal and external regions, the Floquet modes take the form [2]

$$a_{mn} J_{v_m}(k_{\rho n} \rho) + b_{mn} Y_{v_m}(k_{\rho n} \rho) \quad \text{for } \rho < a \quad (2.8.a)$$

and

$$c_{mn} H_{v_m}^{(2)}(k_{\rho n} \rho) + d_{mn} H_{v_m}^{(1)}(k_{\rho n} \rho) \quad \text{for } \rho > a \quad (2.8.b)$$

Here d_{mn} stands for an incoming wave from the external region. All the coefficients of Floquet modes in (2.8.a) and (2.8.b) must be determined from the relevant boundary conditions of the problem. The dispersion relation for the propagation constant $k_{\rho n}$ is

$$k_{\rho n}^2 = k^2 - k_{zn}^2 \quad (2.8.c)$$

Hence for the internal region, we can express any response field U_r by the infinite summation

$$U_r = \sum_{m,n} \left[a_{mn} J_{\nu_m}(k_{\rho n} \rho) + b_{mn} Y_{\nu_m}(k_{\rho n} \rho) \right] \psi_{mn} \quad \text{for } \rho < a \quad (2.9.a)$$

and for the external region by

$$U_T = \sum_{m,n} c_{mn} H_{\nu_m}^{(2)}(k_{\rho n} \rho) \psi_{mn} \quad \text{for } \rho > a \quad (2.9.b)$$

Here the summations are doubly infinite with the indices m, n . The coefficients d_{mn} of (2.8.b) are omitted in (2.9.b), by implicitly assuming that, no wave from the external region is incident.

Hessel [3] gives a proper inner product for these ψ_{mn} harmonics as

$$\langle f, g^* \rangle = \int_{-d/2}^{d/2} \int_{-\alpha/2}^{\alpha/2} f g^* d\phi dz \quad (2.10)$$

One can easily show that, with respect to the inner product (2.10), all Floquet modes ψ_{mn} in (2.7) are orthonormal to each other, i.e.

$$\langle \psi_{mn}, \psi_{rs}^* \rangle = \begin{cases} 1 & \text{for } m=r \quad \text{and} \quad n=s \\ 0 & \text{otherwise} \end{cases} \quad (2.11)$$

Those representations (2.9.a) and (2.9.b), for the cylindrical coordinate system, will be employed in the next Chapters when analyzing periodic cylindrical surfaces.

CHAPTER 3

A TWO DIMENSIONAL DIPOLE ARRAY ON A CYLINDRICAL STRUCTURE

In this chapter, we will consider the periodic cylindrical array of dipoles as shown in Figure 3.1. We will consider this problem since it consists of a periodic cylindrical surface covered with dipoles. Also this periodic surface is excited by an incident field which is periodic in the Floquet sense.

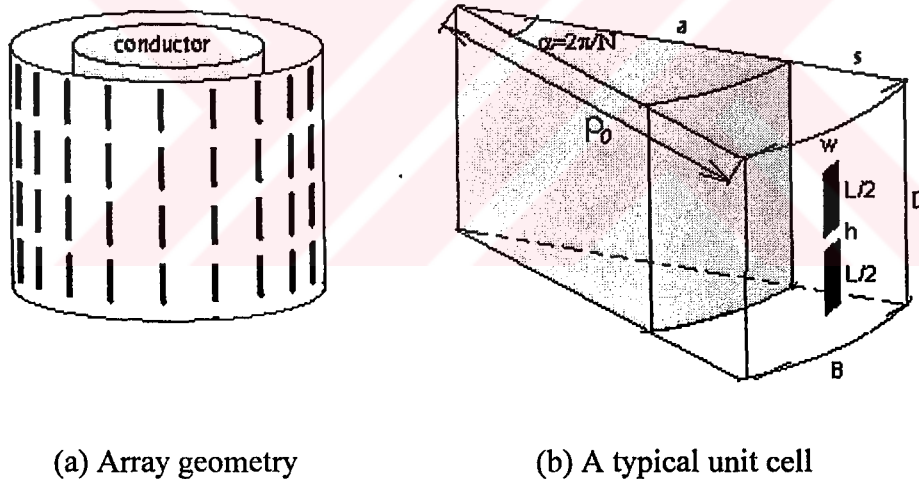


Fig. 3.1. Geometry of the problem

This problem was analyzed by [3] and [4] in 1985, and represents an application of Floquet theorem for a periodic cylindrical surface. So we have included this chapter to give an application of Floquet theorem. Later on Chapter 5, the computer program produced for this work will be modified to calculate the power

reflection and transmission coefficients of our original problem.

We will assume that, all dipoles are excited through their central gaps via transmission lines. Furthermore, we will assume that, all generators maintain voltages that are equal in amplitude but their phases change equally and progressively from element to element. We will call such an excitation as a phase sequence excitation. Then it is very obvious that, for a given phase sequence excitation, the field components radiated from the surface are periodic in the Floquet sense. Therefore the Floquet theorem may be used to express the radiated fields for both internal and external regions.

We will formulate the problem by using the Floquet theorem and evaluate the two important parameters of the surface at the end of the chapter. One of them is the broadside scan gap impedance, which is the impedance seen across the gap of a dipole when all generators are co-phased (zero phase sequence excitation case). The other important parameter is the active element pattern, which is the radiation pattern of a singly excited dipole in an environment where all other dipoles are terminated (all other generators are short-circuited).

3.1. Array Model

The cylindrical array model under consideration, shown in Figure 3.1., consists of an infinite number of equispaced rings of axial dipoles. The rings, of radius ρ_0 , contain N equispaced identical dipoles each located coaxially a distance s above an infinite, perfectly conducting cylindrical surface of radius a . The dipoles have a length L , narrow width W , and negligible radial thickness. Their central gaps of length h are excited through identical matching networks, via transverse electromagnetic (TEM) transmission line feeds from generators. A typical wedge shaped unit cell of axial dimension d and angular width α is seen in the Figure 3.1. The feeding network is not shown in the figure.

3.2. Active Dipole Current

For a phase sequence excitation v_0 in the ϕ direction and k_{z0} in the z direction, the voltage of the $(s,t)^{th}$ dipole gap is given by

$$V_{g,st}(v_0, k_{z0}) = V_{g,00}(v_0, k_{z0})e^{-j(v_0\alpha)s}e^{-j(k_{z0}d)t} \quad (3.1)$$

where $V_{g,00}(v_0, k_{z0})$ represents the voltage of the reference dipole (0,0). Here $(v_0\alpha)$ and $(k_{z0}d)$ are fixed interelement phase shifts in the ϕ and z directions respectively. Such an excitation is periodic in the Floquet sense and the radiated fields can be written as a sum of the Floquet modes. Recall from Chapter 2 that, the Floquet modes for such a periodic surface is given (2.7) as

$$\psi_{mn} = \frac{e^{-jv_m\phi}e^{-jk_{zn}z}}{\sqrt{\alpha d}} \quad (3.2)$$

where

$$v_m = v_0 + \frac{2\pi m}{\alpha} \quad \text{and} \quad k_{zn} = k_{z0} + \frac{2\pi n}{d}$$

and the inner product was defined in (2.10) as

$$\langle f, g^* \rangle = \int_{-d/2}^{d/2} \int_{-\alpha/2}^{\alpha/2} fg^* d\phi dz \quad (3.3)$$

Note that, with respect to the inner product (3.3), all Floquet modes ψ_{mn} are orthonormal to each other.

If the width of a dipole is very narrow in terms of wavelength $w/\lambda \ll 1$, then we can assume axial dipole currents over the surface [3]. As a consequence, all field components may be derived from a single axial component of a magnetic vector potential A_z . Various field components in cylindrical coordinate system, for an electromagnetic vector potential A_z , are

$$E_z = \frac{-j}{\omega\mu_0\epsilon_0} \left[\frac{\partial^2}{\partial z^2} + k_0^2 \right] A_z \quad (3.4.a)$$

$$E_\rho = \frac{-j}{\omega\mu_0\epsilon_0} \left[\frac{\partial^2}{\partial \rho \partial z} \right] A_z \quad (3.4.b)$$

$$E_\phi = \frac{-j}{\omega\mu_0\epsilon_0} \left[\frac{\partial^2}{\partial \phi \partial z} \right] A_z \quad (3.4.c)$$

$$H_\phi = \frac{-1}{\mu_0} \left[\frac{\partial}{\partial \rho} \right] A_z \quad (3.4.d)$$

$$H_\rho = \frac{-1}{\rho} \left[\frac{\partial}{\partial \phi} \right] A_z \quad (3.4.e)$$

$$H_z = 0 \quad (3.4.f)$$

Now the magnetic vector potential A_z for the radiated fields should be written in a series of Floquet modes. Using the Floquet mode summations (2.90.a) and (2.9.b),

$$A_z^I = \sum_{m,n} \left[a_{mn} J_{\nu_m}(k_{\rho n} \rho) + b_{mn} Y_{\nu_m}(k_{\rho n} \rho) \right] \psi_{mn} \quad \text{for } \rho < \rho_0 \quad (3.5.a)$$

and

$$A_z^{II} = \sum_{m,n} c_{mn} H_{\nu_m}^{(2)}(k_{\rho n} \rho) \psi_{mn} \quad \text{for } \rho > \rho_0 \quad (3.5.b)$$

where

$$k_{\rho n}^2 + k_{zn}^2 = k_0^2$$

Note that Bessel functions of the first and second kinds are used in (3.5.a) to represent a standing wave in the internal region. On the other hand Bessel function of the second kind is used in (3.5.b) to represent a propagating wave. Let us note that

the propagation constant $k_{\rho n}$, for each mode in the ρ direction, may be real or purely imaginary. A convenient square root choice is [3]

$$k_{\rho n} = \begin{cases} \sqrt{k_0^2 - k_{zn}^2} & \text{for } k_0^2 > k_{zn}^2 \\ -j\sqrt{k_{zn}^2 - k_0^2} & \text{for } k_0^2 < k_{zn}^2 \end{cases} \quad (3.6)$$

The determination of the unknown coefficients a_{mn} , b_{mn} , and c_{mn} in (3.5) can be made by applying the boundary conditions. The boundary conditions to be satisfied are:

1. The tangential components of radiated electric field over the surface of the conducting cylinder must be zero, i.e.

$$E_z' = E_\phi' = 0 \quad \text{at } \rho = a \quad (3.7.a)$$

2. The tangential components of radiated electric field must be continuous at $\rho = \rho_0$

$$E_z' = E_z'' \quad , \quad E_\phi' = E_\phi'' \quad \text{at } \rho = \rho_0 \quad (3.7.b)$$

3. The tangential components of magnetic field should have a discontinuity at $\rho = \rho_0$ which is equal to the induced current density on the dipole

$$H_\phi'' - H_\phi' = K_z \quad (3.7.c)$$

For the boundary condition (3.7.a), z component of electric field is

$$\begin{aligned} E_z' &= \frac{-j}{\omega\mu_0\epsilon_0} \left[\frac{\partial^2}{\partial z^2} + k_0^2 \right] \sum_{m,n} \left[a_{mn} J_{v_m}(k_{\rho n}\rho) + b_{mn} Y_{v_m}(k_{\rho n}\rho) \right] \psi_{mn} \\ &= \frac{-j}{\omega\mu_0\epsilon_0} \sum_{m,n} k_{\rho n}^2 \left[a_{mn} J_{v_m}(k_{\rho n}\rho) + b_{mn} Y_{v_m}(k_{\rho n}\rho) \right] \psi_{mn} \quad \text{for } \rho < \rho_0 \end{aligned} \quad (3.8)$$

By equation (3.8) to 0 at $\rho = a$ and taking the inner product of both sides by ψ_{mn}^* and by making use of orthonormality property of Floquet modes, we can obtain

$$a_{mn}J_{v_m}(k_{\rho n}a) + b_{mn}Y_{v_m}(k_{\rho n}a) = 0 \quad (3.9)$$

For the boundary condition (3.7.b), z component of electric field for the external region is

$$\begin{aligned} E_z^{\parallel} &= \frac{-j}{\omega\mu_0\epsilon_0} \left[\frac{\partial^2}{\partial z^2} + k_0^2 \right] \sum_{m,n} \left[c_{mn} H_{v_m}^{(2)}(k_{\rho n}\rho) \right] \psi_{mn} \\ &= \frac{-j}{\omega\mu_0\epsilon_0} \sum_{m,n} k_{\rho n}^2 \left[c_{mn} H_{v_m}^{(2)}(k_{\rho n}\rho) \right] \psi_{mn} \quad \text{for } \rho > \rho_0 \end{aligned} \quad (3.10)$$

At $\rho = \rho_0$, the tangential electric field must be continuous. From (3.8) and (3.10) one can find, by making use of orthonormality property of Floquet modes,

$$a_{mn}J_{v_m}(k_{\rho n}\rho_0) + b_{mn}Y_{v_m}(k_{\rho n}\rho_0) = c_{mn}H_{v_m}^{(2)}(k_{\rho n}\rho_0) \quad (3.11)$$

However at $\rho = \rho_0$ the boundary condition (3.7.c) requires, using (3.4.d)

$$\frac{-1}{\mu_0} \left[\frac{\partial}{\partial \rho} A_z^{\parallel} - \frac{\partial}{\partial \rho} A_z^{\prime} \right]_{\rho=\rho_0} = K_z(\rho_0, \phi, z) \quad (3.12)$$

where K_z is defined on the dipole's surface and zero elsewhere. Using (3.5a) and (3.5.b) and taking the inner product of both sides by ψ_{mn}^* and employing the orthonormality property of Floquet modes we may get

$$k_{\rho n} \left[c_{mn} H_{v_m}^{(2)}(k_{\rho n}\rho_0) - \left(a_{mn} J_{v_m}'(k_{\rho n}\rho_0) + b_{mn} Y_{v_m}'(k_{\rho n}\rho_0) \right) \right] = -\mu_0 \langle K_z, \psi_{mn}^* \rangle \quad (3.13)$$

Here the primes denote the differentiation with respect to argument for the Bessel's functions.

The simultaneous solution of (3.9), (3.11), and (3.13) for the unknown coefficients, with the wronskian relation [7], gives

$$c_{mn} = \frac{\pi\mu_0\rho_0}{2j} \langle K_z, \psi_{mn}^* \rangle \left[J_{v_m}(k_{\rho n}\rho_0) - \frac{H_{v_m}^{(2)}(k_{\rho n}\rho_0)}{H_{v_m}^{(2)}(k_{\rho n}a)} J_{v_m}(k_{\rho n}a) \right] \quad (3.14.a)$$

$$b_{mn} = -\frac{\pi\mu_0\rho_0}{2j} \langle K_z, \psi_{mn}^* \rangle \frac{J_{v_m}(k_{\rho_n}a)}{H_{v_m}^{(2)}(k_{\rho_n}a)} H_{v_m}^{(2)}(k_{\rho_n}\rho_0) \quad (3.14.b)$$

$$a_{mn} = -\frac{\pi\mu_0\rho_0}{2j} \langle K_z, \psi_{mn}^* \rangle H_{v_m}^{(2)}(k_{\rho_n}\rho_0) \quad (3.14.c)$$

The boundary condition on the dipole surface requires $E_z^I = E_z^{II} = 0$ on the dipole arms and $E_z^I = E_z^{II} = E_g$ in the gap. Note that E_g is forced dipole gap field associated with the phase sequence excitation (3.1). For the reference element

$$E_g = \begin{cases} -\frac{V_{g,00}(v_0, k_{z0})}{h} & \text{in the gap} \\ 0 & \text{on dipole arms} \end{cases} \quad (3.15)$$

Using (3.10) at $\rho = \rho_0$

$$\frac{-j}{\omega\mu_0\varepsilon_0} \sum_{m,n} k_{\rho_n}^2 c_{mn} H_{v_m}^{(2)}(k_{\rho_n}\rho_0) \psi_{mn} = -E_g \quad (3.16)$$

By using (3.14.a), equation (3.16) can be put into the form

$$\frac{\pi}{2} k_0 Z_0 \rho_0 \sum_{m,n} \left(\frac{k_{\rho_n}}{k_0}\right)^2 \langle K_z, \psi_{mn}^* \rangle \left[J_{v_m}(k_{\rho_n}\rho_0) - \frac{H_{v_m}^{(2)}(k_{\rho_n}\rho_0)}{H_{v_m}^{(2)}(k_{\rho_n}a)} J_{v_m}(k_{\rho_n}a) \right] H_{v_m}^{(2)}(k_{\rho_n}\rho_0) \psi_{mn} = E_g \quad (3.17)$$

where

$$Z_0 = \sqrt{\frac{\mu_0}{\varepsilon_0}} = 120\pi$$

This final equation is an operator type equation in the form

$$L\{K_z\} = E_g \quad (3.18)$$

in which E_g is a known exciting function given by (3.15) and (3.1), and K_z is a response current which is an unknown yet. One of the convenient method to solve

such an equation is the method of moments [5]. Once the integral equation is solved for K_z all radiated field components can be found by using the field equations (3.4)

3.3. Method Of Moments

If we expand the current in the form

$$K_z = \sum_{q=1}^Q c_q \tilde{\Psi}_q \quad (3.19)$$

and choose the basis functions [3] as

$$\tilde{\Psi}_q(\phi, z) = \begin{cases} \sin\left[\frac{q\pi}{L}\left(z + \frac{L}{2}\right)\right] & \text{on dipole arms} \\ 0 & \text{elsewhere} \end{cases} \quad (3.20)$$

the operator equation (3.18) becomes

$$\sum_{q=1}^Q c_q L(\tilde{\Psi}_q) = E_g \quad (3.21)$$

Relation (3.21) is enforced by taking inner product of both sides with each of $\tilde{\Psi}_p$. This procedure yields the desired set of linear equations for the unknown set of c_q , i.e.,

$$\sum_{q=1}^Q c_q \langle \tilde{\Psi}_p, L(\tilde{\Psi}_q) \rangle = \langle \tilde{\Psi}_p, E_z' \rangle, \quad p = 1, 2, \dots, Q \quad (3.22)$$

The inner product under the summation of (3.22) is, from (3.17), (3.18), and (3.19),

$$\begin{aligned} \langle \tilde{\Psi}_p, L(\tilde{\Psi}_q) \rangle &= \left\langle \tilde{\Psi}_p, \frac{\pi}{2} k_0 Z_0 \rho_0 \sum_{m,n} \left(\frac{k_{\rho m}}{k_0}\right)^2 \langle \tilde{\Psi}_q, \psi_{mn}^* \rangle \right. \\ &\quad \left. \left[J_{\nu_m}(k_{\rho n} \rho_0) - \frac{H_{\nu_m}^{(2)}(k_{\rho n} \rho_0)}{H_{\nu_m}^{(2)}(k_{\rho n} a)} J_{\nu_m}(k_{\rho n} a) \right] H_{\nu_m}^{(2)}(k_{\rho n} \rho_0) \psi_{mn} \right\rangle \end{aligned} \quad (3.23)$$

But since for an inner product

$$\left\langle h, \sum_{k=-\infty}^{\infty} a_k f_k \right\rangle = \sum_{k=-\infty}^{\infty} a_k \langle h, f_k \rangle \quad (3.24)$$

(3.23) becomes

$$\begin{aligned} \langle \tilde{\Psi}_p, L(\tilde{\Psi}_q) \rangle &= \frac{\pi}{2} k_0 Z_0 \rho_0 \sum_{m,n} \left(\frac{k_{\rho m}}{k_0} \right)^2 \left[J_{v_m}(k_{\rho m} \rho_0) - \frac{H_{v_m}^{(2)}(k_{\rho m} \rho_0)}{H_{v_m}^{(2)}(k_{\rho m} a)} J_{v_m}(k_{\rho m} a) \right] \\ &H_{v_m}^{(2)}(k_{\rho m} \rho_0) \langle \tilde{\Psi}_q, \psi_{mn}^* \rangle \langle \tilde{\Psi}_p, \psi_{mn} \rangle \end{aligned} \quad (3.25)$$

One can find from (3.3), (3.2), and (3.20) that

$$\begin{aligned} \langle \tilde{\Psi}_q, \psi_{mn}^* \rangle &= \int_{-L/2}^{L/2} \int_{-W/2\rho_0}^{W/2\rho_0} \sin\left[\frac{q\pi}{L}\left(z + \frac{L}{2}\right)\right] \frac{e^{+jv_m\phi} e^{+jk_m z}}{\sqrt{\alpha d}} d\phi dz \\ &= \frac{W\pi L}{\rho_0 \sqrt{\alpha d}} S_{v_m} C_{nq}^* \end{aligned} \quad (3.26)$$

where

$$S_{v_m} = \frac{\sin[v_m W/2\rho_0]}{[v_m W/2\rho_0]} \quad (3.27.a)$$

$$C_{nq}^* = q \frac{[(-1)^q e^{jk_m L/2} - e^{-jk_m L/2}]}{(k_m L)^2 - (q\pi)^2} \quad (3.27.b)$$

Also note that

$$\langle \tilde{\Psi}_p, \psi_{mn} \rangle = \left[\langle \tilde{\Psi}_p, \psi_{mn}^* \rangle \right]^* = \frac{W\pi L}{\rho_0 \sqrt{\alpha d}} S_{v_m} C_{np} \quad (3.28)$$

The right hand side term of (3.22) is, from (3.3), (3.15), and (3.20),

$$\begin{aligned} \langle \tilde{\Psi}_p, E_g \rangle &= \int_{-h/2}^{h/2} \int_{-W/2\rho_0}^{W/2\rho_0} -\frac{V_{g,00}(v_0, k_{z0})}{h} \sin\left[\frac{p\pi}{L}\left(z + \frac{L}{2}\right)\right] d\phi dz \\ &= -\frac{V_{g,00}(v_0, k_{z0})W}{\rho_0} B_p \end{aligned} \quad (3.29)$$

where

$$B_p = \sin\left[\frac{p\pi}{L}\right] \frac{\sin\left[\frac{p\pi h}{2L}\right]}{\left[\frac{p\pi h}{2L}\right]} \quad (3.30)$$

If we let

$$\left[J_{\nu_m}(k_{\rho m} \rho_0) - \frac{H_{\nu_m}^{(2)}(k_{\rho m} \rho_0)}{H_{\nu_m}^{(2)}(k_{\rho m} a)} J_{\nu_m}(k_{\rho m} a) \right] = Z_{\nu_m} \quad (3.31)$$

and use (3.26) and (3.28), the expression (3.25) become simpler

$$\langle \tilde{\Psi}_p, L(\tilde{\Psi}_q) \rangle = \frac{\pi k_0 Z_0 W^2 \pi^2 L^2}{2 \rho_0 \alpha d} \sum_{m,n} \left(\frac{k_{\rho m}}{k_0}\right)^2 Z_{\nu_m} H_{\nu_m}^{(2)}(k_{\rho m} \rho_0) S_{\nu_m}^2 C_{nq}^* C_{np} \quad (3.32)$$

and the set of equations in (3.22) together with (3.29) can be written as

$$\sum_{q=1}^Q c_q \frac{\pi k_0 Z_0 W^2 \pi^2 L^2}{2 \rho_0 \alpha d} \sum_{m,n} \left(\frac{k_{\rho m}}{k_0}\right)^2 Z_{\nu_m} H_{\nu_m}^{(2)}(k_{\rho m} \rho_0) S_{\nu_m}^2 C_{nq}^* C_{np} = -\frac{V_{g,00}(v_0, k_{z0}) W}{\rho_0} B_p \quad (3.33)$$

$p = 1, 2, \dots, Q$

Note that

$$\alpha = \frac{2\pi}{N}$$

where N is the number of elements in a ring. So the equations (3.33) can be written in the form

$$\sum_{q=1}^Q (W \bar{c}_q) A_{pq} = B_p \quad , \quad p = 1, 2, \dots, Q \quad (3.34)$$

where

$$\bar{c}_q = \frac{\pi^2 k_0 Z_0 L^2 N}{4d V_{g,00}(v_0, k_{z0})} c_q \quad (3.35)$$

and

$$A_{pq} = \sum_{m,n} \left(\frac{k_m}{k_0} \right)^2 Z_{v_m} H_{v_m}^{(2)}(k_{\rho m} \rho_0) S_{v_m}^2 C_{nq}^* C_{np} \quad (3.36)$$

3.4. Active Gap Impedance

When the matrix equation (3.34) is solved for the unknowns \bar{c}_q , the current K_z can be written from (3.19), (3.20), and (3.35). The active gap impedance can now be determined via

$$Z_g(v_0, k_{z0}) = R_g(v_0, k_{z0}) + jX_g(v_0, k_{z0}) = \frac{V_{g,00}(v_0, k_{z0})}{\langle I_g \rangle} \quad (3.37)$$

where $\langle I_g \rangle$ denotes the average gap current

$$\begin{aligned} \langle I_g \rangle &= \frac{W}{h} \int_{-h/2}^{h/2} K_z dz = \frac{W}{h} \sum_{q=1}^Q c_q \int_{-h/2}^{h/2} \sin\left[\frac{q\pi}{L} \left(z + \frac{L}{2}\right)\right] dz \\ &= W \sum_{q=1}^Q c_q \sin\left[\frac{q\pi}{2}\right] \frac{\sin[q\pi h / 2L]}{[q\pi h / 2L]} = \sum_{q=1}^Q W c_q B_q \\ &= \frac{4dV_{g,00}(v_0, k_{z0})}{\pi^2 k_0 Z_0 L^2 N} \sum_{q=1}^Q W \bar{c}_q B_q \end{aligned} \quad (3.38)$$

Therefore, from (3.38) and (3.37)

$$Z_g(v_0, k_{z0}) = \frac{N\pi^2 L^2 k_0 Z_0}{4d \sum_{q=1}^Q W \bar{c}_q B_q} \quad (3.39)$$

For a good radiation efficiency, [3] had incorporated an identical matching network in each transmission line to match the dipole impedance $Z_g(v_0, k_{z0})$ for a selected pair of values of v_0 and k_{z0} . [3] explains the matching procedures with more details but they are not included here since it is out of concern for us in the following chapters. We now proceed to find the active array fields to find the element pattern.

3.5. Active Array Fields

From (3.10), (3.14.a), (3.19), (3.26), (3.31), and (3.35) one finds for $\rho > \rho_0$ the axial component of the electric field of the active array

$$E_z^H(v_0, k_{z0}) = \frac{-V_{g,00}(v_0, k_{z0})}{\pi L} \sum_{m,n} \left(\frac{k_{\rho m}}{k_0}\right)^2 \left[\sum_{q=1}^Q W \bar{c}_q C_{nq}^* \right] S_{v_m} Z_{v_m} H_{v_m}^{(2)}(k_{\rho m} \rho) e^{-j(v_m \phi + k_{z0} z)} \quad (3.40)$$

or (3.40) can be written as

$$E_z^H(v_0, k_{z0}) = \frac{-1}{\pi L} \sum_{m,n} T_{mn}^z(v_0, k_{z0}) H_{v_m}^{(2)}(k_{\rho m} \rho) e^{-j(v_m \phi + k_{z0} z)} \quad (3.41)$$

where

$$T_{mn}^z(v_0, k_{z0}) = V_{g,00}(v_0, k_{z0}) \left(\frac{k_{\rho m}}{k_0}\right)^2 \left[\sum_{q=1}^Q W \bar{c}_q C_{nq}^* \right] S_{v_m} Z_{v_m} \quad (3.42)$$

When the dipoles on a single ring are excited and all other dipoles on other ring are match terminated (generators are short circuited), then the axial component of the electric field can be found from the following integration [3]

$$\xi_z^H(v_0, \rho, \phi, z) = \frac{d}{2\pi} \int_{-\pi/d}^{\pi/d} E_z^H(v_0, k_{z0}) dk_{z0} \quad (3.43)$$

which may also be thought as an inverse Fourier transform. Using (3.41) in (3.43)

$$\xi_z^H(v_0, \rho, \phi, z) = \frac{-jd}{2\pi^2 L} \int_{-\pi/d}^{\pi/d} \sum_{m,n} T_{mn}^z(v_0, k_{z0}) H_{v_m}^{(2)}(k_{\rho m} \rho) e^{-j(v_m \phi + k_{z0} z)} dk_{z0} \quad (3.44)$$

Exact solutions of the integral in (3.44) is not possible [3] but for large values of $k_{\rho m} \rho$ the method of stationary phase is applicable [6]. That method gives the far field solution

$$\xi_z^{II}(v_0, \rho, \phi, z) = \frac{jd}{\pi^2 L} \frac{e^{-jk_z r}}{r} \sum_{m=-\infty}^{\infty} e^{-jv_m(\phi-\pi/2)} T_{m0}^z(v_0, k_0 \cos\theta) \quad (3.45)$$

where

$$r = \sqrt{\rho^2 + z^2}, \quad \theta = \arctan(\rho/z)$$

On the other hand, the following summation

$$\xi_z^{II}(\rho, \phi, z) = \frac{1}{N} \sum_{v_0=0}^{N-1} \xi_z^{II}(v_0, r, \phi, z) \quad (3.46)$$

gives the fields radiated from the reference dipole, when all other dipoles are match terminated [3]. Also in spherical coordinate system, the θ -component of electric field is

$$\xi_\theta^{II} = \frac{\xi_z^{II}}{\sin\theta} \quad (3.47)$$

Hence, by using (3.42), (3.45), (3.46), and (3.47)

$$\xi_\theta^{II}(r, \theta, \phi) = \frac{-jd}{\pi^2 L} \frac{e^{-jk_z r}}{r} \sin\theta \sum_{v_0=0}^{N-1} \frac{V_{g,00}(v_0, k_0 \cos\theta)}{N} \sum_{m=-\infty}^{\infty} e^{-jv_m(\phi-\pi/2)} S_{v_m} Z_{v_m} \left[\sum_{q=1}^Q (W\bar{c}_q) C_{0q}^* \right] \quad (3.48)$$

Reference [3] says that the lowest order term of ξ_θ is $O(1/r^2)$ so that the ξ_θ contribution to the far field may be omitted. Consequently, ξ_θ contributes the entire far electric field due to a singly excited dipole element in a match terminated environment [3].

The gap voltage $V_{g,00}(v_0, k_0 \cos\theta)$ of (3.48), after a proper matching network, is given in terms of the generator voltage V_{inc} [3] as

$$V_{g,00}(v_0, k_{z0}) = \sqrt{\frac{R_g(0,0)}{Z_1}} \frac{2Z_g(v_0, k_{z0})}{Z_g(v_0, k_{z0}) + Z_g^*(0,0)} V_{inc} \quad , \quad k_{z0} = k_0 \cos\theta \quad (3.49)$$

where $Z_g^*(0,0)$ denotes the complex conjugate of the broadside scan gap impedance (the impedance seen across the gap of a dipole when $v_0 = k_{z0} = 0$) and Z_1 is the characteristic impedance of transmission line.

The element gain pattern is defined by

$$G_\theta^e(\theta, \phi) = \frac{|\xi_\theta''(r, \theta, \phi)|^2}{Z_0} \frac{4\pi r^2}{P_{inc}} \quad (3.50)$$

where P_{inc} represents the power that would be supplied by the generator if the transmission line was match terminated. The characteristic impedance of the transmission line is chosen in (3.49) as Z_1 , therefore

$$P_{inc} = \frac{|V_{inc}|^2}{Z_1} \quad (3.51)$$

Hence by using (3.48), (3.49), and (3.51) in (3.50) we can obtain

$$G_\theta^e(\theta, \phi) = \frac{16d^2 \sin^2 \theta R_g(0,0)}{Z_0 N^2 L^2 \pi^3} \left[\sum_{v_0=0}^{N-1} \frac{Z_g(v_0, k_0 \cos\theta)}{Z_g(v_0, k_0 \cos\theta) + Z_g^*(0,0)} \sum_{m=-\infty}^{\infty} e^{-jv_m(\phi - \pi/2)} S_{v_m} Z_{v_m} \left[\sum_{q=1}^Q (W\bar{c}_q) C_{0q}^* \right] \right]^2 \quad (3.52)$$

Here $G_\theta^e(\theta, \phi)$ represents the element pattern of an axial dipole in a match terminated environment, i.e., only the reference dipole is excited by a generator and all other generators are short-circuited.

3.6. Numerical Analysis

Based on the analysis of this chapter, a Fortran program is generated for

evaluation of the dipole surface current coefficients c_q , and for the evaluation of the phase sequence active gap impedances $Z_g(v_0, k_0 \cos\theta)$.

The Bessel functions of the matrix elements A_{pq} in (3.36) were evaluated by the numerical methods described in [7], each applicable in its own range of validity with respect to argument and order. The slow convergence of the infinite summations in A_{pq} was accelerated as described in Appendix B. With such convergence acceleration, modal indices m and n between ± 10 were used for the evaluation of the matrix elements.

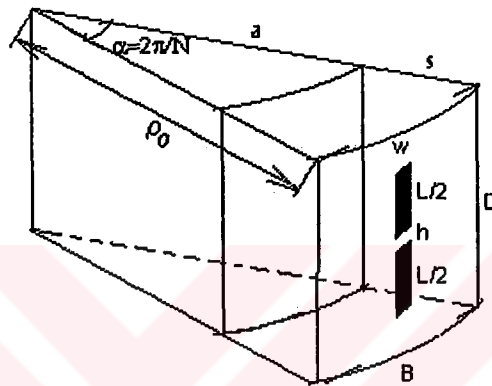


Fig. 3.2. Unit cell geometry

For the figure 3.2., following set of parameters were used in calculations

$$\rho_0 = (120 / 2\pi + 0.25)\lambda$$

$$a = (120 / 2\pi)\lambda$$

$$s = 0.25\lambda$$

$$L = 0.5\lambda$$

$$W = 0.05\lambda$$

$$h = 0.01\lambda$$

$$d = 0.7\lambda$$

$$N = 200$$

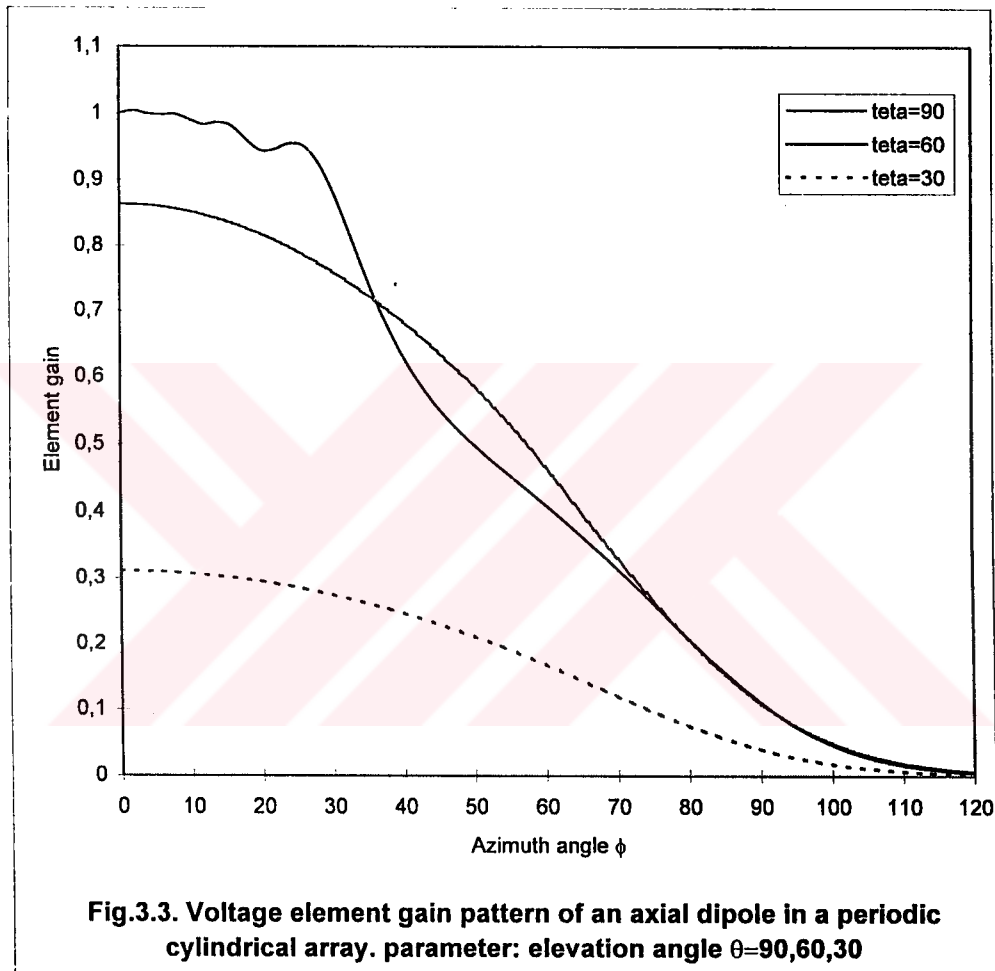
$$Q = 10$$

Firstly the broadside scan gap impedance $Z_g(0,0)$ [(3.52)] is calculated

to be

$$Z_r(0,0) = 104.16 - j5.883\Omega \quad (3.53)$$

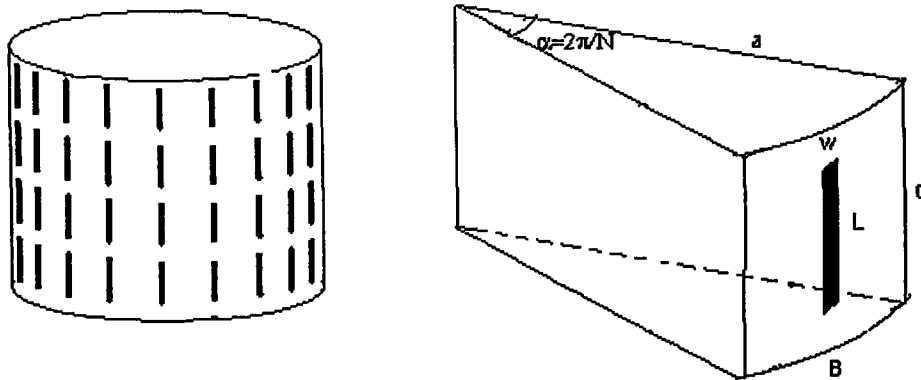
Then the element gain pattern [(3.49)] is computed from which the graph in figure 3.3. is produced. Figure 3.3. shows the element pattern features as a function of the elevation angle at $\theta = 30^\circ, 60^\circ, 90^\circ$ cuts. As seen with decreasing values of θ the gain level is progressively reduced.



CHAPTER 4

A CYLINDRICAL FREQUENCY SELECTIVE SURFACE

In this chapter, an infinite cylindrical array is considered that consists of metal strips arranged periodically as shown in Figure 4.1. All the strips in the array are assumed to be identical and infinitesimally thin. Such a surface was analyzed in Chapter 3 but the strips were excited by voltage generators via transmission lines. Here the excitation is considered to be a cylindrical wave which is incident from the internal region at any oblique angle and periodic in the Floquet sense. By employing the Floquet theorem, the surface is analyzed for the reflection and transmission coefficients.



(a) Array geometry

(b) A typical unit cell

Fig. 4.1. A cylindrical surface covered periodically with metal strips

The procedure to be presented here is to expand the electromagnetic field distribution near the array of the metal strips into a set of Floquet mode functions. By requiring the total electric field to vanish over the strips, an integral equation for the unknown current on each strip is obtained. To solve this integral equation the unknown current is first expressed by a complete set of orthonormal mode functions and then its mode coefficients are determined by the method of moments. At the end of the chapter, the reflection and transmission coefficients are expressed in terms of the mode coefficients.

4.1. Passive Array Currents

The frequency selective surface given in the figure consists of an infinite number of periodically arranged axial metal strips. The radius of the surface is a and each ring contains N metal strips. The length and the width of a strip are L and W respectively.

To begin with, one observes that for

$$\frac{W}{\lambda} \ll 1 \quad (4.1)$$

an axial current K_z should yield a good approximation for the induced currents. As a consequence, all field components may be derived from a single axial component of a vector potential A_z .

The incident wave is assumed to be radiated from a current filament lying along z axis. If the current filament has a constant amplitude I_0 and a linear phase variation k_{z0} along z axis, then the radiated magnetic field is (see appendix A)

$$H_\phi = \frac{jk_{\rho 0} I_0}{4} H_0^{(2)}(k_{\rho 0} \rho) e^{-jk_{z0} z} \quad (4.2)$$

which is periodic in the Floquet sense, i.e., it has a constant amplitude and a linear

phase change in z direction at $\rho = a$ and has no variation with respect to ϕ . For such a periodic excitation, the Floquet modes are (see Chapter 2)

$$\Psi_{mn} = \frac{e^{-jv_m\phi} e^{-jk_{zn}z}}{\sqrt{\alpha d}} \quad (4.3)$$

where

$$v_m = v_0 + \frac{2\pi m}{\alpha} = \frac{2\pi m}{\alpha} = mN, \quad k_{zn} = k_{z0} + \frac{2\pi n}{d} \quad m, n = 0, \pm 1, \pm 2, \pm 3, \dots$$

$$k_{\rho n}^2 = k_0^2 - k_{zn}^2$$

and the inner product is defined as

$$\langle f, g^* \rangle = \int_{-d/2-\alpha/2}^{d/2-\alpha/2} \int f g^* d\phi dz \quad (4.4)$$

The propagation constant $k_{\rho n}$ is a double valued function of its argument. A convenient square root choice is [3]

$$k_{\rho n} = \begin{cases} \sqrt{k_0^2 - k_{zn}^2} & \text{for } k_0^2 > k_{zn}^2 \\ -j\sqrt{k_{zn}^2 - k_0^2} & \text{for } k_0^2 < k_{zn}^2 \end{cases}$$

For the external and internal regions, convenient representations for the scattered magnetic vector potential A_z are (see Chapter 2)

$$A_z^{\text{II}} = \sum_{m,n} a_{mn} H_{v_m}^{(2)}(k_{\rho n} \rho) \Psi_{mn} \quad \text{for } \rho > a \quad (4.5)$$

$$A_z^{\text{I}} = \sum_{m,n} b_{mn} J_{v_m}(k_{\rho n} \rho) \Psi_{mn} \quad \text{for } \rho < a \quad (4.6)$$

Here Hankel function of the second kind is chosen for (4.5) to represent outgoing waves in the external region. But only Bessel function of the first kind is chosen in (4.6) since the field should be finite at the origin. The determination of a_{mn} and b_{mn} can be made by applying the boundary conditions at $\rho = a$.

Various field components in cylindrical coordinate system are

$$E_z = \frac{-j}{\omega\mu_0\epsilon_0} \left[\frac{\partial^2}{\partial z^2} + k_0^2 \right] A_z \quad (4.7.a)$$

$$E_\rho = \frac{-j}{\omega\mu_0\epsilon_0} \left[\frac{\partial^2}{\partial\rho\partial z} \right] A_z \quad (4.7.b)$$

$$E_\phi = \frac{-j}{\omega\mu_0\epsilon_0} \left[\frac{\partial^2}{\partial\phi\partial z} \right] A_z \quad (4.7.c)$$

$$H_\phi = \frac{-1}{\mu_0} \left[\frac{\partial}{\partial\rho} \right] A_z \quad (4.7.d)$$

$$H_\rho = \frac{-1}{\rho} \left[\frac{\partial}{\partial\phi} \right] A_z \quad (4.7.e)$$

$$H_z = 0 \quad (4.7.f)$$

At $\rho = a$ the tangential components of electric field must be continuous

$$E_z^I = E_z^{II} \quad \text{and} \quad E_\phi^I = E_\phi^{II} \quad \text{at} \quad \rho = a \quad (4.8)$$

From (4.5), (4.6) and (4.7.a), the z component of electric fields for the external and internal region are, respectively

$$E_z^{II} = \frac{-j}{\omega\mu_0\epsilon_0} \sum_{m,n} k_{\rho n}^2 a_{mn} H_{v_m}^{(2)}(k_{\rho n}\rho) \psi_{mn} \quad \text{for} \quad \rho > a \quad (4.9)$$

$$E_z^I = \frac{-j}{\omega\mu_0\epsilon_0} \sum_{m,n} k_{\rho n}^2 b_{mn} J_{v_m}(k_{\rho n}\rho) \psi_{mn} \quad \text{for} \quad \rho < a \quad (4.10)$$

Hence by using the boundary condition (4.8) for the fields (4.9) and (4.10), we can write

$$\sum_{m,n} k_{\rho n}^2 \left[a_{mn} H_{v_m}^{(2)}(k_{\rho n}a) - b_{mn} J_{v_m}(k_{\rho n}a) \right] \psi_{mn} = 0 \quad (4.11)$$

Taking the inner product of (4.11) with ψ_{mn}^* and using the orthonormality property of Floquet modes, we can write

$$a_{mn} H_{v_m}^{(2)}(k_{\rho n} a) - b_{mn} J_{v_m}(k_{\rho n} a) = 0 \quad (4.12)$$

However the tangential component of the magnetic field should be discontinuous by an amount equal to the induced current density K_z

$$K_z = H_{\phi}^{II} - H_{\phi}^I \quad \text{at} \quad \rho = a \quad (4.13)$$

From (4.5), (4.6) and (4.7.d), the ϕ component of magnetic fields for the external and internal region are, respectively

$$H_{\phi}^{II} = \frac{-1}{\mu_0} \sum_{m,n} k_{\rho n} a_{mn} H_{v_m}^{(2)}(k_{\rho n} \rho) \psi_{mn} \quad \text{for} \quad \rho > a \quad (4.14)$$

$$H_{\phi}^I = \frac{-1}{\mu_0} \sum_{m,n} k_{\rho n} b_{mn} J_{v_m}(k_{\rho n} \rho) \psi_{mn} \quad \text{for} \quad \rho < a \quad (4.15)$$

where primes on Bessel functions denote differentiation with respect to argument. By using the boundary condition (4.13) for the fields (4.14) and (4.15)

$$K_z = \frac{-1}{\mu_0} \sum_{m,n} k_{\rho n} \left[a_{mn} H_{v_m}^{(2)}(k_{\rho n} a) - b_{mn} J_{v_m}'(k_{\rho n} a) \right] \psi_{mn} \quad (4.16)$$

If we take the inner product of both sides of (4.16) by ψ_{mn}^* and use the orthonormality property of Floquet modes, we obtain

$$k_{\rho n} \left[a_{mn} H_{v_m}^{(2)}(k_{\rho n} a) - b_{mn} J_{v_m}'(k_{\rho n} a) \right] = -\mu_0 \langle K_z, \psi_{mn}^* \rangle \quad (4.17)$$

Simultaneous solution of the equations (4.12) and (4.17), after employing the wronskian relation, gives

$$a_{mn} = \frac{-j}{2} \pi a \mu_0 \langle K_z, \psi_{mn}^* \rangle J_{v_m}(k_{\rho n} a) \quad (4.18)$$

$$b_{mn} = \frac{-j}{2} \pi a \mu_0 \langle K_z, \psi_{mn}^* \rangle H_{v_m}^{(2)}(k_{\rho n} a) \quad (4.19)$$

The boundary condition on a strip surface requires

$$E_z^i + E_z^{II} = E_z^i + E_z^I = 0 \quad \text{on strip surface} \quad (4.20)$$

where E_z^i is the incident field which is radiated from an internal current filament of amplitude I_0 and given by (see appendix A)

$$E_z^i = -\left(\frac{k_{\rho n}}{k_0}\right)^2 \frac{k_0 Z_0 I_0}{4} H_0^{(2)}(k_{\rho 0} \rho) e^{-jk_z z} \quad (4.21)$$

The boundary condition (4.20) gives an electric field integral equation (EFIE) for the problem. If we use E_z^{II} for the boundary condition (4.20), then from (4.9) we can obtain

$$\frac{-j}{\omega \mu_0 \epsilon_0} \sum_{m,n} k_{\rho n}^2 a_{mn} H_{v_m}^{(2)}(k_{\rho n} a) \psi_{mn} = -E_z^i \quad \text{on } S_{strip}$$

or by using (4.18), we can write

$$\frac{\pi}{2} k_0 Z_0 a \sum_{m,n} \left(\frac{k_{\rho n}}{k_0}\right)^2 \langle K_z, \psi_{mn}^* \rangle J_{v_m}(k_{\rho n} a) H_{v_m}^{(2)}(k_{\rho n} a) \psi_{mn} = E_z^i \quad \text{on } S_{strip} \quad (4.22)$$

where

$$Z_0 = \sqrt{\frac{\mu_0}{\epsilon_0}} = 120\pi$$

4.2. Moment Method Matrix Equation

The electric field integral equation (4.22) is an operator type equation in the form

$$L\{K_z\} = E_z^i \quad \text{over } S_{strip} \quad (4.23)$$

If we expand the current in the form

$$K_z = \sum_{q=1}^Q c_q \tilde{\Psi}_q \quad (4.24)$$

and choose the basis functions as [3]

$$\tilde{\Psi}_q(\phi, z) = \begin{cases} \sin\left[\frac{q\pi}{L}\left(z + \frac{L}{2}\right)\right] & \text{over } S_{strip} \\ 0 & \text{elsewhere} \end{cases} \quad (4.25)$$

then the operator equation (4.23) becomes

$$\sum_{q=1}^Q c_q L(\tilde{\Psi}_q) = E_z^i \quad (4.26)$$

Also if we take the inner product of both sides of (4.26) with $\tilde{\Psi}_p$, we obtain

$$\sum_{q=1}^Q c_q \langle \tilde{\Psi}_p, L(\tilde{\Psi}_q) \rangle = \langle \tilde{\Psi}_p, E_z^i \rangle, \quad p = 1, 2, \dots, Q \quad (4.27)$$

which is a set of Q equations with Q unknowns. The inner product term under the summation of (4.27) can be written more explicitly from (4.22) and (4.23) that

$$\langle \tilde{\Psi}_p, L(\tilde{\Psi}_q) \rangle = \left\langle \tilde{\Psi}_p, \frac{\pi}{2} k_0 Z_0 a \sum_{m,n} \left(\frac{k_{\rho n}}{k_0}\right)^2 \langle \tilde{\Psi}_q, \psi_{mn}^* \rangle J_{\nu_m}(k_{\rho n} a) H_{\nu_m}^{(2)}(k_{\rho n} a) \psi_{mn} \right\rangle \quad (4.28)$$

The position of the infinite summation and the inner product can be interchanged since one can write the identity

$$\left\langle h, \sum_{k=-\infty}^{\infty} a_k f_k \right\rangle = \sum_{k=-\infty}^{\infty} a_k \langle h, f_k \rangle \quad (4.29)$$

So the expression (4.28) becomes

$$\langle \tilde{\Psi}_p, L(\tilde{\Psi}_q) \rangle = \frac{\pi}{2} k_0 Z_0 a \sum_{m,n} \left(\frac{k_{\rho n}}{k_0}\right)^2 J_{\nu_m}(k_{\rho n} a) H_{\nu_m}^{(2)}(k_{\rho n} a) \langle \tilde{\Psi}_q, \psi_{mn}^* \rangle \langle \tilde{\Psi}_p, \psi_{mn} \rangle \quad (4.30)$$

The inner products of (4.30) can be written as, by using the definitions of the inner product (4.4) and the basis functions (4.25),

$$\langle \tilde{\Psi}_p, \Psi_{mn} \rangle = \int_{-L/2}^{L/2} \int_{-W/2a}^{W/2a} \sin\left[\frac{p\pi}{L}\left(z + \frac{L}{2}\right)\right] \frac{e^{-jv_m\phi} e^{-jk_m z}}{\sqrt{\alpha d}} d\phi dz = \frac{W\pi L}{a\sqrt{\alpha d}} S_{v_m} C_{np} \quad (4.31)$$

where

$$S_{v_m} = \frac{\sin[v_m W/2a]}{[v_m W/2a]} \quad (4.32.a)$$

$$C_{np} = p \frac{[(-1)^p e^{-jk_m L/2} - e^{jk_m L/2}]}{(k_m L)^2 - (p\pi)^2} \quad (4.32.b)$$

Also, from the results (4.31), (4.32.a), (4.32.b) we can write

$$\langle \tilde{\Psi}_q, \Psi_{mn}^* \rangle = \left[\langle \tilde{\Psi}_q, \Psi_{mn} \rangle \right]^* = \frac{W\pi L}{a\sqrt{\alpha d}} S_{v_m} C_{nq}^* \quad (4.33)$$

The right hand side inner product operation of (4.27) is, from the definitions (4.4) and (4.25)

$$\langle \tilde{\Psi}_p, E_z^i \rangle = \int_{-L/2}^{L/2} \int_{-W/2a}^{W/2a} E_z^i|_{\rho=a} \sin\left[\frac{p\pi}{L}\left(z + \frac{L}{2}\right)\right] d\phi dz \quad (4.34)$$

Note that from (4.21) we can write

$$E_z^i = -\left(\frac{k_{\rho 0}}{k_0}\right)^2 \frac{k_0 Z_0 J_0}{4} H_0^{(2)}(k_{\rho 0} a) \sqrt{\alpha d} \psi_{00} \quad \text{at } \rho = a \quad (4.35)$$

and (4.34) becomes, after using the result of (4.31)

$$\langle \tilde{\Psi}_p, E_z^i \rangle = -\left(\frac{k_{\rho 0}}{k_0}\right) \frac{k_0 Z_0 J_0}{4} H_0^{(2)}(k_{\rho 0} a) \sqrt{\alpha d} \frac{W\pi L}{a\sqrt{\alpha d}} S_{v_0} C_{0p} = B_p \quad (4.36)$$

Hence by using the results (4.30), (4.31), (4.33), (4.36), the set of equations (4.27) becomes

$$\sum_{q=1}^Q c_q \frac{\pi}{2} k_0 Z_0 a \sum_{m,n} \left(\frac{k_m}{k_0}\right)^2 J_{\nu_m}(k_{\rho m} a) H_{\nu_m}^{(2)}(k_{\rho m} a) \frac{W\pi L}{a\sqrt{\alpha d}} S_{\nu_m} C_{nq}^* \frac{W\pi L}{a\sqrt{\alpha d}} S_{\nu_m} C_{np} = B_p \quad (4.37)$$

Finally we can write the expression (4.37) as

$$\sum_{q=1}^Q \bar{c}_q A_{pq} = B_p \quad , \quad p = 1, 2, \dots, Q \quad (4.38)$$

where

$$\bar{c}_q = \frac{\pi k_0 Z_0 W^2 \pi^2 L^2}{2\alpha\alpha d} c_q \quad (4.39)$$

and

$$A_{pq} = \sum_{m,n} \left(\frac{k_m}{k_0}\right)^2 C_{nq}^* C_{np} S_{\nu_m}^2 J_{\nu_m}(k_{\rho m} a) H_{\nu_m}^{(2)}(k_{\rho m} a) \quad (4.40)$$

Matrix elements A_{pq} are evaluated by using the usual numerical methods for the Bessel functions, each applicable in its own range of validity with respect to the argument and order [7]. The doubly infinite summation of A_{pq} can be calculated in the form $\sum_n g_n \sum_m f_{mn}$ and the following observations are relevant:

a) The series $\sum_n g_n$ converges as $\frac{1}{n^3}$

b) The series $\sum_m f_{mn}$ converges as $\frac{1}{2\pi^2|m|}$

The slow convergence of $\sum_m f_{mn}$ is accelerated as described in Appendix B. The set of equations are solved for the unknown current coefficients c_q , using Gauss's elimination method.

4.3. Reflection And Transmission Coefficients

In this section, surface reflection and transmission coefficients will be written in terms of the current coefficients c_q .

Let us note that, if a surface current density \vec{J}_s radiates the electric field \vec{E}^r , then the following integral

$$P = - \iint_S \vec{E}^r \bullet \vec{J}_s^* ds \quad (4.41)$$

gives the total complex power radiated by that surface current [2]. Here S represents the surface over which the current is flowing. Also the real part of P gives the time average radiated power

$$P_{av} = \text{Re} \left\{ - \iint_S \vec{E}^r \bullet \vec{J}_s^* ds \right\} \quad (4.42)$$

In our problem, an incident field E_z^i induces current density K_z on each strip. In turn, that induced current density radiates the scattered fields \vec{E}^I and \vec{E}^{II} to the internal and external regions respectively. Hence

$$P^I = - \iint_S (\vec{E}^I) \bullet (\vec{a}_z K_z^*) ds = \int_{-L/2}^{L/2} \int_{-W/2a}^{W/2a} E_z^I K_z^* (-ad\phi dz) \quad (4.43)$$

gives the total complex power radiated back into the region I by each strip. The integration of (4.43) is equivalent to the inner product operation

$$P^I = -a \langle E_z^I, K_z^* \rangle \quad (4.44)$$

which is obvious from (4.4). By using (4.10) for (4.44)

$$\begin{aligned}
P^I &= -a \left\langle \frac{-j}{\omega \mu_0 \epsilon_0} \sum_{m,n} k_{\rho n}^2 b_{mn} J_{v_m}(k_{\rho n} a) \psi_{mn}, K_z^* \right\rangle \\
&= \frac{ja}{\omega \mu_0 \epsilon_0} \sum_{m,n} k_{\rho n}^2 b_{mn} J_{v_m}(k_{\rho n} a) \langle \psi_{mn}, K_z^* \rangle
\end{aligned} \tag{4.45}$$

If we recall b_{mn} from (4.19), we can write

$$\begin{aligned}
P^I &= \frac{ja}{\omega \mu_0 \epsilon_0} \sum_{m,n} k_{\rho n}^2 \frac{-j}{2} \pi a \mu_0 H_{v_m}^{(2)}(k_{\rho n} a) J_{v_m}(k_{\rho n} a) \langle K_z, \psi_{mn}^* \rangle \langle \psi_{mn}, K_z^* \rangle \\
&= \frac{a^2 \pi}{2 \omega \epsilon_0} \sum_{m,n} k_{\rho n}^2 H_{v_m}^{(2)}(k_{\rho n} a) J_{v_m}(k_{\rho n} a) \langle K_z, \psi_{mn}^* \rangle^2
\end{aligned} \tag{4.46}$$

Now the real part of (4.46) gives the time average power radiated by each strip. But since

$$H_{v_m}^{(2)}(k_{\rho n} a) J_{v_m}(k_{\rho n} a) = \left| J_{v_m}(k_{\rho n} a) \right|^2 - j Y_{v_m}(k_{\rho n} a) J_{v_m}(k_{\rho n} a)$$

the real part of (4.46) is

$$P_{av}^I = \frac{a^2 \pi}{2 \omega \epsilon_0} \sum_{m,n} k_{\rho n}^2 \left| J_{v_m}(k_{\rho n} a) \right|^2 \langle K_z, \psi_{mn}^* \rangle^2 \tag{4.47}$$

Recall from (4.24) that

$$K_z = \sum_{q=1}^Q c_q \tilde{\Psi}_q$$

so that we can write

$$\langle K_z, \psi_{mn}^* \rangle = \left\langle \sum_{q=1}^Q c_q \tilde{\Psi}_q, \psi_{mn}^* \right\rangle = \sum_{q=1}^Q c_q \langle \tilde{\Psi}_q, \psi_{mn}^* \rangle$$

or from (4.33) we obtain

$$\langle K_z, \psi_{mn}^* \rangle = \frac{W \pi L}{a \sqrt{\alpha d}} \sum_{q=1}^Q c_q S_{v_m} C_{nq}^* = \frac{W \pi L}{a \sqrt{\alpha d}} S_{v_m} \sum_{q=1}^Q c_q C_{nq}^* \tag{4.48}$$

Hence the time average power reflected by each strip becomes, by using (4.48) in (4.47),

$$\begin{aligned}
P_{av}^I &= \frac{a^2 \pi}{2\omega \epsilon_0} \frac{W^2 \pi^2 L^2}{a^2 \alpha d} \sum_{m,n} k_{\rho n}^2 \left| J_{\nu_m}(k_{\rho n} a) \right|^2 S_{\nu_m}^2 \left| \sum_{q=1}^Q c_q C_{nq}^* \right|^2 \\
&= \frac{\pi W^2 \pi^2 L^2}{2\omega \epsilon_0 \alpha d} \sum_{n=-\infty}^{\infty} k_{\rho n}^2 \left| \sum_{q=1}^Q c_q C_{nq}^* \right|^2 \sum_{m=-\infty}^{\infty} S_{\nu_m}^2 \left| J_{\nu_m}(k_{\rho n} a) \right|^2
\end{aligned} \tag{4.49}$$

If we divide this power with

$$P_{inc} = \left(\frac{k_{\rho 0}}{k_0} \right)^2 \frac{k_0 Z_0}{4} \alpha d \tag{4.50}$$

which is the power incident per unit cell (see appendix A), we obtain the surface power reflection coefficient

$$\begin{aligned}
|\Gamma|^2 &= \frac{4k_0^2}{k_{\rho 0}^2 k_0 Z_0 \alpha d} P_{av}^I \\
&= \frac{2\pi W^2 \pi^2 L^2}{\alpha^2 d^2 k_{\rho 0}^2} \sum_{n=-\infty}^{\infty} k_{\rho n}^2 \left| \sum_{q=1}^Q c_q C_{nq}^* \right|^2 \sum_{m=-\infty}^{\infty} S_{\nu_m}^2 \left| J_{\nu_m}(k_{\rho n} a) \right|^2
\end{aligned} \tag{4.51}$$

In order to find an expression for the power transmission coefficient in view of (4.41), following division

$$|T|^2 = \frac{-\operatorname{Re} \left\{ \iint_S (\vec{E}^i + \vec{E}^r) \cdot \vec{J}_i^* ds \right\}}{-\operatorname{Re} \left\{ \iint_S \vec{E}^i \cdot \vec{J}_i^* ds \right\}} \tag{4.52}$$

may be used. Here \vec{J}_i represents the impressed line current density (see appendix A)

$$\vec{J}_i^* = \hat{a}_z I_z^* = \hat{a}_z I_0 e^{+jk_0 z} \quad \text{at } \rho = 0 \tag{4.53}$$

and S represents the surface of a cylinder with an infinitesimal radius. Obviously, the denominator term of (4.52) represents the power that would be radiated by the impressed current (4.53) if the surface was not present. On the other hand, the

numerator term of (4.52) represents the total power radiated from the same impressed current (4.53) to infinity in presence of the scatterers. Taking the limit of (4.52) and using (4.53), we can write

$$|T|^2 = 1 + \lim_{\rho \rightarrow 0} \left(\frac{\operatorname{Re} \left\{ \iint_S E_z' I_z^* ds \right\}}{\operatorname{Re} \left\{ \iint_S E_z' I_z^* ds \right\}} \right) \quad (4.54)$$

If we choose the boundary of a unit cell, α and d , for the surface S in (4.54) and use $ds = \rho d\phi dz$

$$|T|^2 = 1 + \lim_{\rho \rightarrow 0} \left(\frac{\operatorname{Re} \left\{ \int_{-d/2}^{d/2} \int_{-\alpha/2}^{\alpha/2} E_z' I_z^* \rho d\phi dz \right\}}{\operatorname{Re} \left\{ \int_{-d/2}^{d/2} \int_{-\alpha/2}^{\alpha/2} E_z' I_z^* \rho d\phi dz \right\}} \right) = 1 + \frac{\operatorname{Re} \left\{ \int_{-d/2}^{d/2} \int_{-\alpha/2}^{\alpha/2} E_z'(\rho=0) I_z^* d\phi dz \right\}}{\lim_{\rho \rightarrow 0} \operatorname{Re} \left\{ \int_{-d/2}^{d/2} \int_{-\alpha/2}^{\alpha/2} E_z' I_z^* d\phi dz \right\}} \quad (4.55)$$

The integrations of (4.55) are equivalent to the definition of inner product (4.4). So we can write

$$|T|^2 = 1 + \frac{\operatorname{Re} \left\{ \langle E_z'(\rho=0), I_z^* \rangle \right\}}{\lim_{\rho \rightarrow 0} \operatorname{Re} \left\{ \langle E_z', I_z^* \rangle \right\}} \quad (4.56)$$

Also one may write from (4.53) that, for $I_0 = 1$,

$$I_z^* = e^{+jk_z z} = \sqrt{\alpha d} \psi_{00}^* \quad (4.57)$$

Now if we consider the inner product of (4.10) and (4.57) for the numerator term of (4.56), and use the orthonormality property of Floquet modes

$$\begin{aligned} \operatorname{Re} \left\{ \langle E_z'(\rho=0), I_z^* \rangle \right\} &= \operatorname{Re} \left\{ \left\langle \frac{-j}{\omega \mu_0 \epsilon_0} \sum_{m,n} k_{\rho n}^2 b_{mn} J_{v_m}(0) \psi_{mn}, \sqrt{\alpha d} \psi_{00}^* \right\rangle \right\} \\ &= \operatorname{Re} \left\{ \frac{-j \sqrt{\alpha d} k_{\rho 0}^2 b_{00}}{\omega \mu_0 \epsilon_0} \right\} = \frac{\sqrt{\alpha d} k_{\rho 0}^2}{\omega \mu_0 \epsilon_0} \operatorname{Re} \left\{ -j b_{00} \right\} \end{aligned} \quad (4.58)$$

Similarly, by considering the inner product of (4.21) and (4.57) for the denominator term of (4.56)

$$\begin{aligned} \lim_{\rho \rightarrow 0} \left\{ \operatorname{Re} \left\{ \left\langle E'_z, I_z^* \right\rangle \right\} \right\} &= \lim_{\rho \rightarrow 0} \left\{ \operatorname{Re} \left\{ \left\langle - \left(\frac{k_{\rho 0}}{k_0} \right)^2 \frac{k_0 Z_0}{4} H_0^{(2)}(k_{\rho 0} \rho) \sqrt{\alpha d} \psi_{00}, \sqrt{\alpha d} \psi_{00}^* \right\rangle \right\} \right\} \\ &= \lim_{\rho \rightarrow 0} \left\{ \operatorname{Re} \left\{ - \left(\frac{k_{\rho 0}}{k_0} \right)^2 \frac{k_0 Z_0}{4} H_0^{(2)}(k_{\rho 0} \rho) \alpha d \right\} \right\} = - \left(\frac{k_{\rho 0}}{k_0} \right)^2 \frac{k_0 Z_0 \alpha d}{4} \end{aligned} \quad (4.59)$$

Hence by using (4.58) and (4.59) in (4.56) we can obtain

$$|T|^2 = 1 - \frac{4k_0 \operatorname{Re}\{-jb_{00}\}}{Z_0 \omega \mu_0 \varepsilon_0 \sqrt{\alpha d}} \quad (4.60)$$

or by using (4.19)

$$\operatorname{Re}\{-jb_{00}\} = \frac{-\pi \mu_0 W \pi L}{2\sqrt{\alpha d}} S_0 \operatorname{Re} \left\{ \left[\sum_{q=1}^Q c_q C_{0q}^* \right] H_0^{(2)}(k_{\rho 0} a) \right\}$$

the equation (4.60) can be written as

$$|T|^2 = 1 + \frac{2\pi W \pi L}{\alpha d} S_0 \operatorname{Re} \left\{ \left[\sum_{q=1}^Q c_q C_{0q}^* \right] H_0^{(2)}(k_{\rho 0} a) \right\} \quad (4.61)$$

Hence we have obtained two expressions (4.51) and (4.61) for the power reflection and transmission coefficients, in terms of the complex current coefficients c_q . Once the matrix equation (4.38) is solved for c_q , then the power reflection and transmission coefficients can be calculated and the conservation of power can be tested from

$$|T|^2 + |\Gamma|^2 = 1 \quad (4.62)$$

In the next chapter, the conservation of power (4.62) is used as a check for the accuracy of the numerical results.

CHAPTER 5

NUMERICAL RESULTS

Based on the analysis of Chapter 4, a Fortran program is generated to find the power reflection and transmission coefficients of a cylindrical frequency selective surface as a function of frequency. The expression (4.51) and (4.61) are used in calculations.

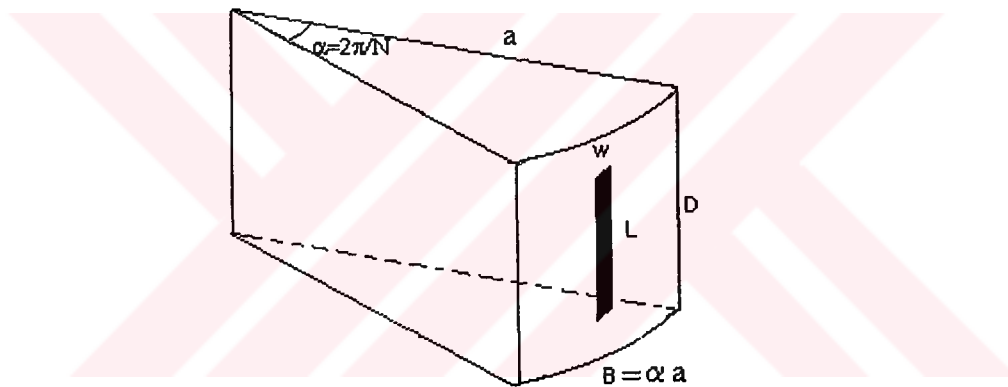


Fig. 5.1. Unit cell geometry

The geometry of a unit cell is shown in Figure 5.1. The induced current over the metal strip is expressed as a sum of 10 sine functions given in (4.25). Also, to match the boundary conditions, 400 Floquet modes are used in calculations.

5.1. Some Representative Calculations

In all results given in this section we assume

$$\frac{W}{\lambda_0} \ll 1 \quad (5.1)$$

for all frequency ranges given in figures or else our initial axial strip current

assumption would not hold. In our calculations we use the following set

$$W = 5mm$$

$$L = 50mm$$

$$B = 60mm$$

$$d = D = 70mm$$

$$N = 200 \text{elements} / \text{ring}$$

$$\alpha = 2\pi / N$$

$$a = B / \alpha = BN / (2\pi)$$

Shown in Figure 5.2. is the variation of the power reflection and transmission coefficients as a function of frequency when the surface is illuminated by a normally incident cylindrical wave with H field perpendicular to z axis. As seen in the figure, the bandwidth increases with the strip width. But the resonance frequency, where the transmission becomes zero, does not change with the strip width. For all values of W, the structure resonates at 2.93GHz.

In the Figure 5.3., power reflection and transmission coefficients are given for different values of strip length L for the normal incidence case. It can be seen from the figure that the resonance frequency decreases as we increase the strip length. In addition, with an increase in the strip length L, the bandwidth also increases slightly.

Figure 5.4. shows the power reflection and transmission response of the surface for different values of unit cell length D. We note that the band width decreases with increasing unit cell length. On the other hand, the resonance frequency approximately remains constant for all values of D.

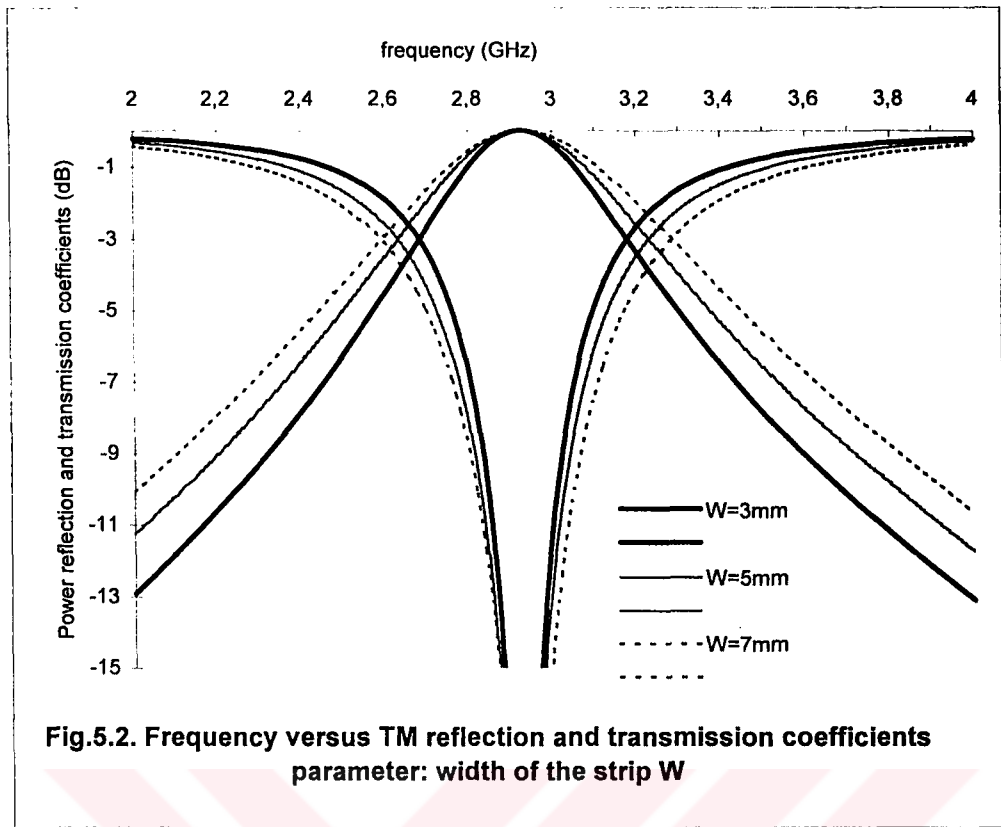
The Figure 5.5. illustrates surface performance for the changes of unit cell width B for a cylindrical wave incident normally. As seen in the figure, surface reflection and transmission characteristics are very sensitive to the changes in unit cell width. For B=70mm resonance frequency is 2.82GHz and the bandwidth is narrow. But if we decrease B to 50mm, resonance frequency becomes 3.05GHz and the bandwidth increases.

In the Figure 5.6. power reflection and transmission coefficients are

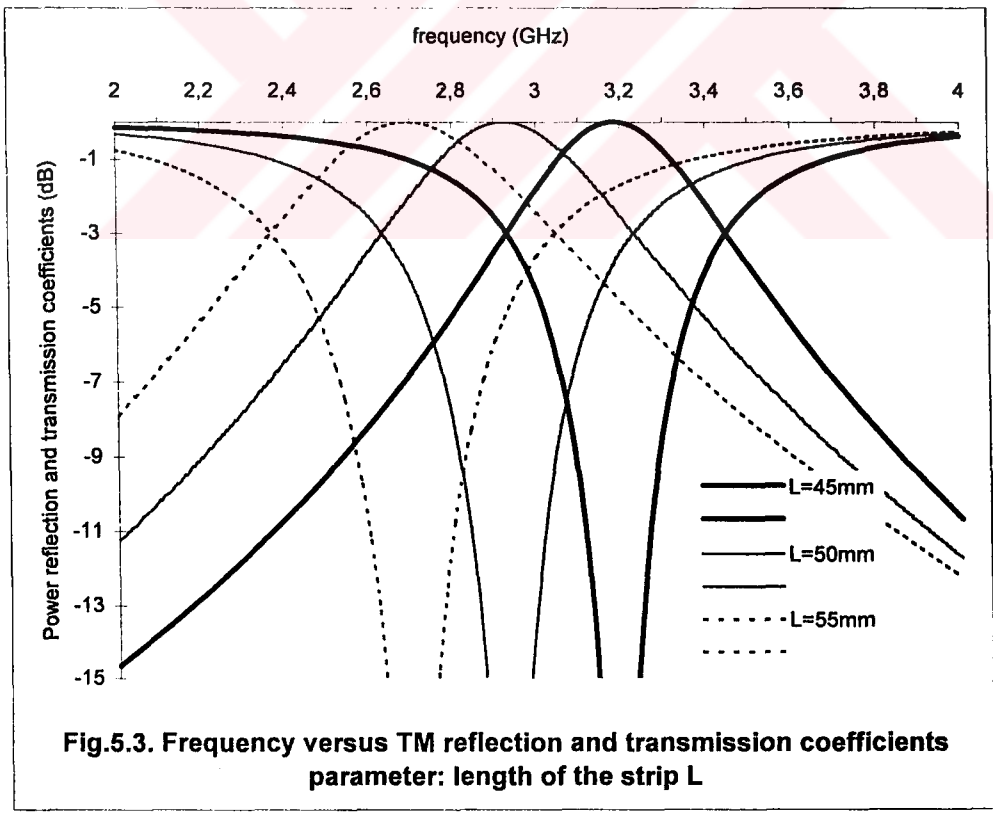
calculated for different number of elements N , for normal incidence case. As seen in the figure, if we increase the number of elements in the array, the resonance frequency and the bandwidth also increase. On the other hand, if we use less elements in the array, the resonance frequency decreases and the bandwidth becomes very narrow.

Figure 5.7. shows the reflection and transmission coefficients of the surface for a cylindrical wave with H field perpendicular to z axis, incident at angles $\theta_0 = 45^\circ, 60^\circ$, and 90° . It is seen that the resonance frequency decreases very slowly, as the angle of incidence is changed from 90° to 60° . But after 60° the resonance frequency approximately remains constant. Also it is seen that the bandwidth is nearly insensitive to the angle of incidence.

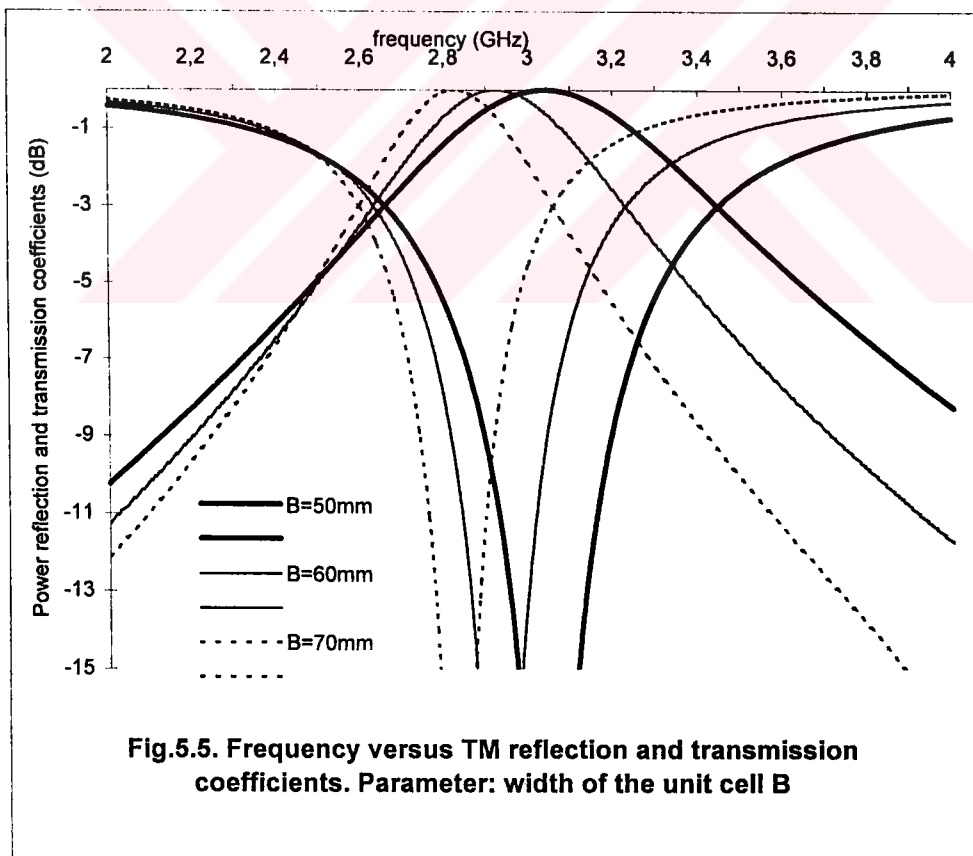
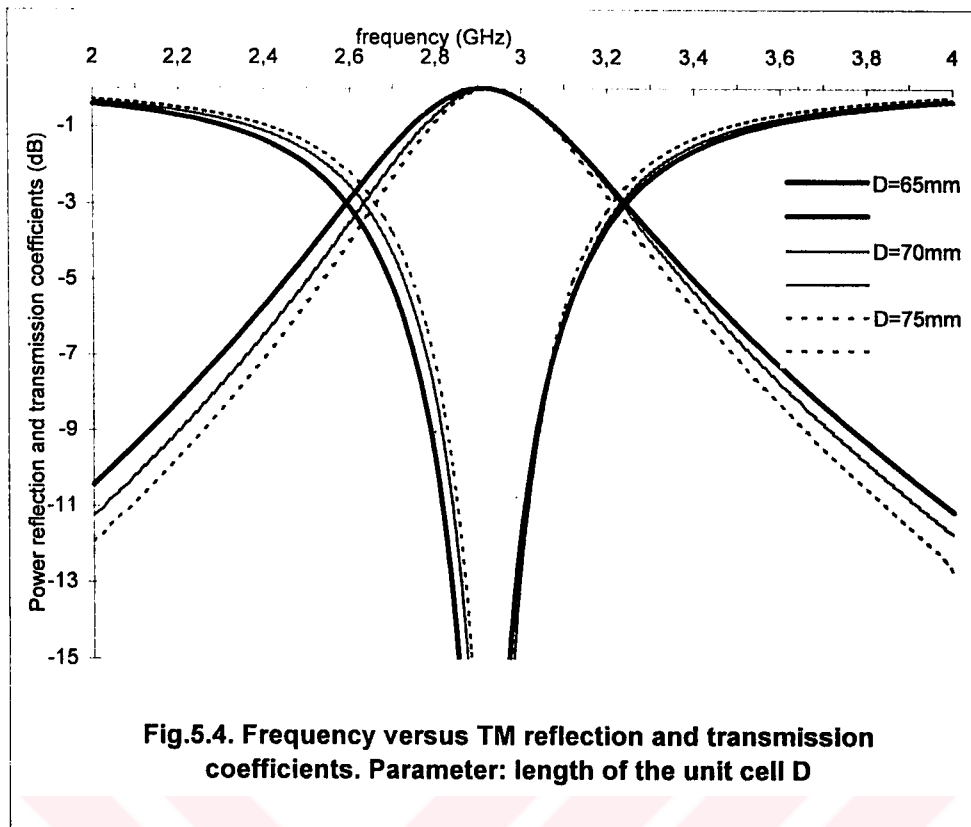
The graph in Figure 5.8 shows the frequency response of the surface for different strip length values $L=45\text{mm}, 50\text{mm}, 55\text{mm}$ when the angle of incidence is $\theta_0 = 60^\circ$. The behavior is similar to the normal incidence case of Figure 5.3 but the resonance frequencies of $\theta_0 = 90^\circ$ case are higher.

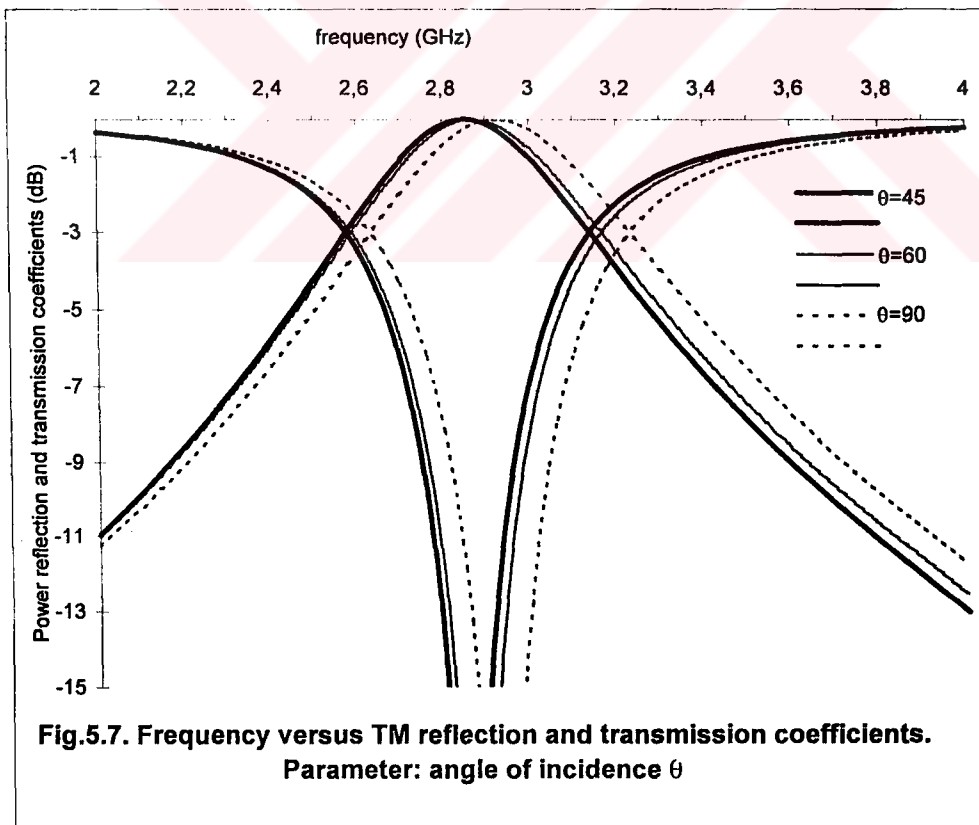
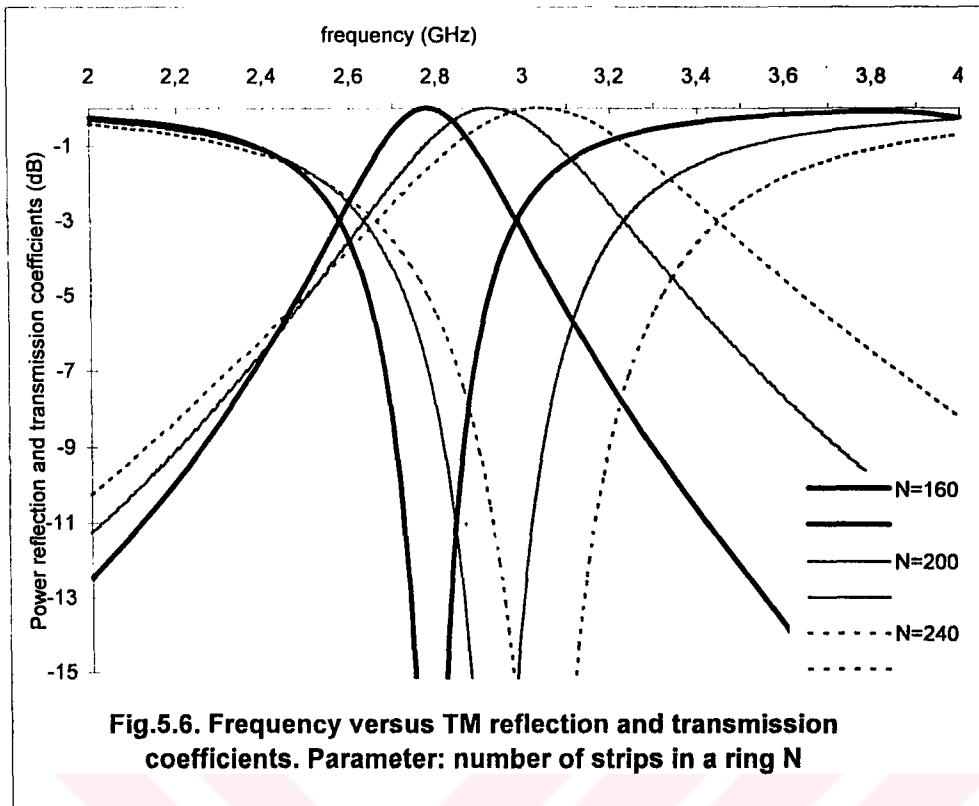


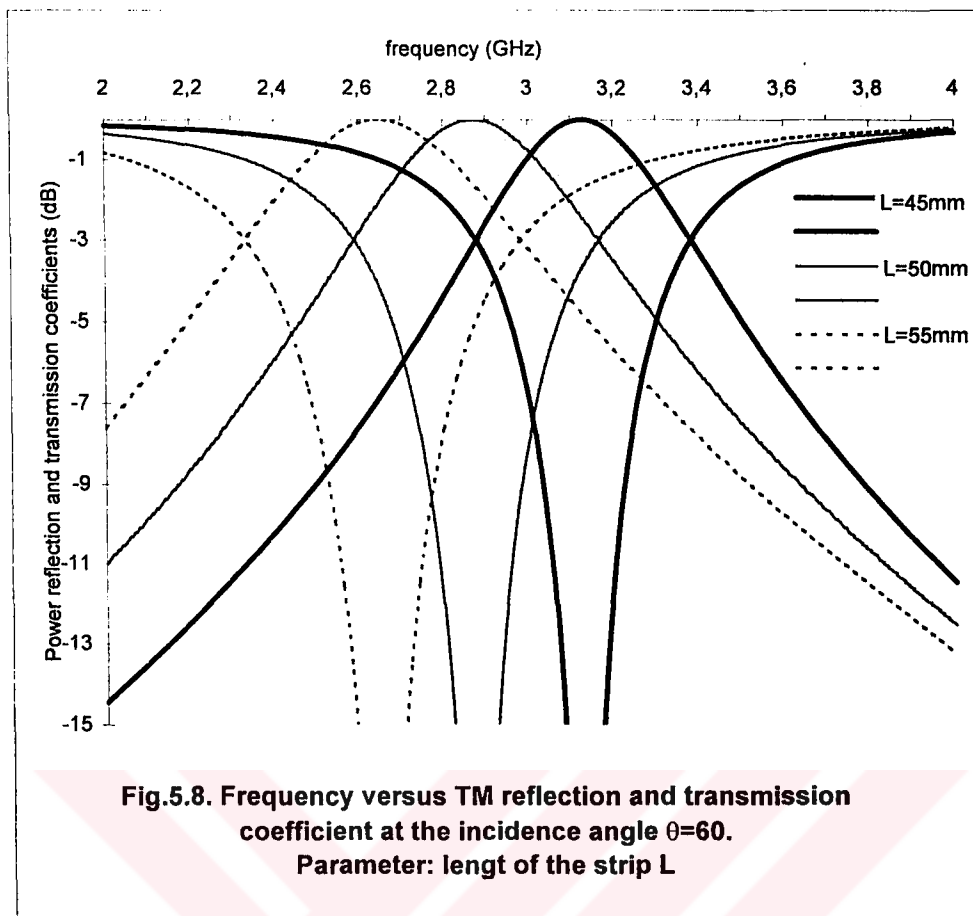
**Fig.5.2. Frequency versus TM reflection and transmission coefficients
parameter: width of the strip W**



**Fig.5.3. Frequency versus TM reflection and transmission coefficients
parameter: length of the strip L**







5.2. Comparison With Other Results

No reference is found in the literature for a two dimensional cylindrical frequency selective surface. In this section we have used the results of a planar frequency selective surface geometry analyzed by [9] and [10] to compare our results. In [10], periodic array of axial strips on a plane was analyzed by using entire domain basis functions to represent induced current on each strip as we do in Chapter 4. Later, [9] have analyzed the same problem by using subdomain basis functions.

In the reference [9], a planar frequency selective surface has been analyzed for a normally incident TM plane wave for the parameter set

$$W = 2.38mm$$

$$L = 13.3mm$$

$$D = 15.2mm$$

$$B = 7.6mm$$

Here B, D are rectangular periodicities over the planar surface and W, L are the strip dimensions. Using this parameter set for the unit cell geometry of Figure 5.1. and taking $N=200$, we considered a normally incident cylindrical wave to a cylindrical surface and plotted the power reflection coefficient with respect to frequency as shown in Figure 5.9. The result of [9] is also cited for comparison. As seen from the figure, the agreement is excellent. Note that near the resonance frequency $f_0 = 14GHz$ the radius of our cylindrical surface in terms of wavelength becomes

$$\frac{a}{\lambda_0} = \frac{BN}{2\pi\lambda_0} \cong 11.29$$

But the geometry of [9] had been previously analyzed by [10] in 1970 by using entire domain basis functions to represent induced current on each strip. In [10], the periodicity of the surface B and D are the same but the strip dimensions are $W=1.27mm$ and $L=13.5mm$. Hence by using

$$W = 1.27mm$$

$$L = 13.5mm$$

$$D = 15.2mm$$

$$B = 7.6mm$$

and taking $N=200$ for the geometry Figure 5.1., we calculated the reflection coefficient of a normally incident cylindrical wave as shown in Figure 5.10. Also the result of [10] is cited for comparison. As seen in the figure resonance frequencies are the same exactly, but the bandwidth of cylindrical surface is wider. Near the resonance frequency $f_0 = 12.8GHz$ the radius of the cylindrical surface, in terms of wavelength is

$$\frac{a}{\lambda_0} = \frac{BN}{2\pi\lambda_0} \cong 10.32$$

As seen from these two figures, agreements between our cylindrical frequency selective surface and its counter part are good.

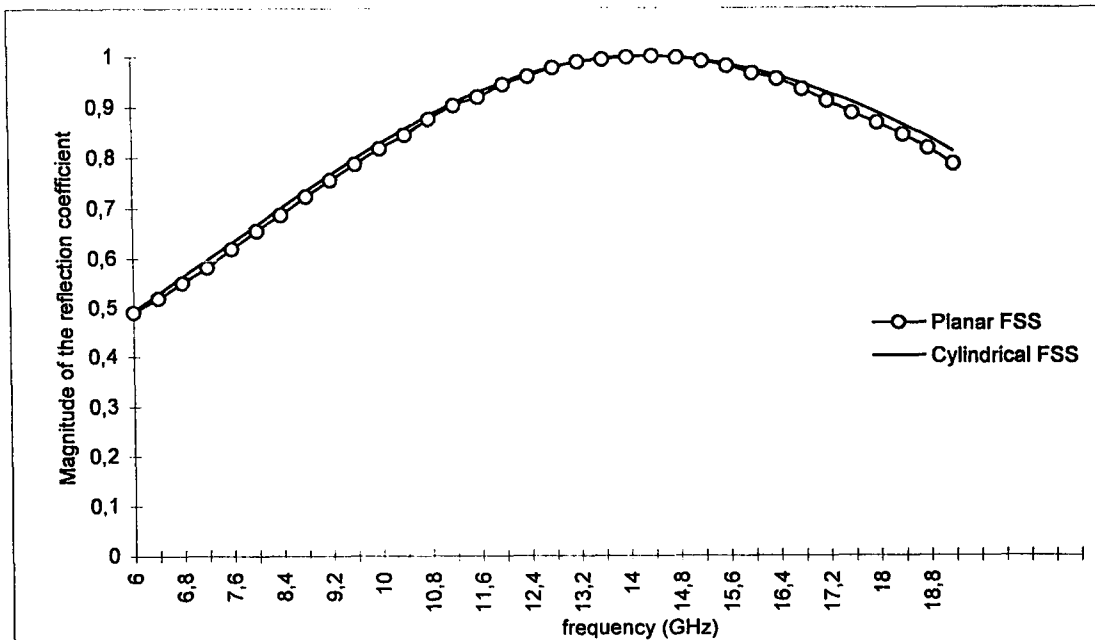


Fig.5.9. Comparison to planar FSS given in [9]

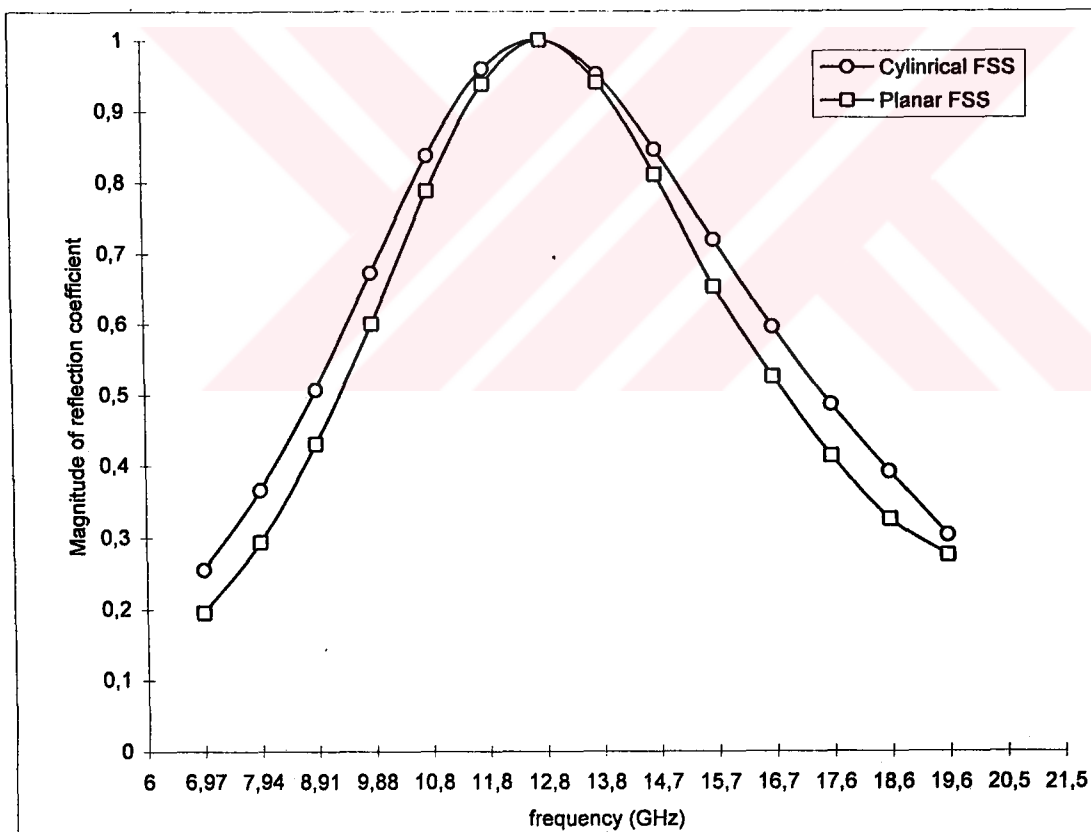


Fig.5.10. Comparison to planar FSS given in [10]

CHAPTER 6

CONCLUSION

In this thesis, a cylindrical frequency selective surface covered periodically with axial metal strips were analyzed for the reflection and transmission coefficients. The assumption of very narrow width for the strips reduced the complexity of the problem and hence the numerical analysis.

The results obtained show that:

a) The resonance frequency of the surface is insensitive to the strip width W . The unit cell length D and the angle of incidence have also relatively minor effects on the resonating frequency. On the other hand, the length of the strip, the width of the unit cell α , and the curvature of the array (number of elements in a ring) strongly effect the resonance frequency.

b) The bandwidth of the reflection or transmission coefficients is sensitive to the strip width W , unit cell length D , unit cell width B and the curvature of the array. The length of the strip L and the angle of incidence effect the bandwidth negligibly.

In this work we analyzed a TM^z incidence case. For a TE^z incidence case, ϕ component of electric field would induce ϕ directed currents on each axial strip. But since the strips are very narrow, those induced currents would be negligible. As a result no power would be scattered by the strips and the surface would be transparent to the incident wave for all frequencies. A similar problem to our work would be a periodic arrangement circumferential strips over a cylindrical surface. For such a

problem, ϕ component of incident electric field would induce ϕ directed current over each strip and each strip would radiate the scattered fields.

A dual problem to our work is a periodic arrangement of axial slots over a perfectly conducting cylinder. One may also analyze the problem of circumferential slots over a perfectly conducting cylinder.



REFERENCES

1. "Electromagnetic Wave Radiation, Propagation and Scattering", Akira Ishimaru, 1991.
2. Tom Cwick, "Coupling into and scattering from cylindrical structures covered periodically with metallic patches", IEEE Transactions on Antennas and Propagation, pp. 220-226, Feb 1990.
3. J. C. Herper, A. Hessel and B. Tomasic, "Element pattern of an axial dipole in a cylindrical phased array- Theory and Experiment", IEEE Transactions on Antennas and Propagation, pp. 259-272, March 1985
4. J. C. Herper, A. Hessel and B. Tomasic, "Element pattern of an axial dipole in a cylindrical phased array- Theory and Experiment", RADC Rep., 1985.
5. "Field Computation by Moment Methods", Roger F. Harrington, 1968.
6. "Asymptotic Analysis", J. D. Murray, 1974.
7. "Handbook of mathematical functions", Milton Abramowitz and Irena A. Stegun, 1965.
8. "Time harmonic electromagnetic fields", Roger F. Harrington, 1961.
9. Chi. Hou. Chan and R. Mittra, "On the analysis of frequency selective surfaces using subdomain basis functions", IEEE Transactions on Antennas and Propagation. pp. 40-50, January 1990.
10. C. C. Chan, "Scattering by a two dimensional periodic array of conducting plates", IEEE Transactions on Antennas and Propagation. pp. 661-665, September 1970.

11. R. Mittra, C. H. Chan, T. Cwick, "Techniques for analyzing frequency selective surfaces—A Review", *Proceedings of IEEE*, vol. 76, N. 12, pp. 1593-1614, December 1988.
12. I. Sato, S. Tamugava, and R. Iwata, "Broadbanding of rectangular metallic mesh quasi-optical diplexer by brick arrangements of apertures", *IEEE Int. Antennas Propagat. Soc. Symp.*, pp. 933-936, Boston, MASS, June 1984.
13. S. Contu, and D. Savini, "Coupled dichroic surfaces for close operating frequency bands", *IEEE Int. Antennas Propagat. Soc. Symp.*, pp. 929-932, Boston, MASS, June 1984.
14. H. Onta, K. C. Lang, and R. Mittra, "Design of two screen frequency selective surface for C/Ku-band satellite communication", *IEEE Int. Antennas Propagat. Soc. Symp.*, pp. 357-360, Houston, TX, May 1983.
15. C. A. Chen, and C. C. Chen, "Wideband sharp frequency cut-off dichroic reflectors for 44/20 GHz application", *IEEE Int. Antennas Propagat. Soc. Symp.*, pp. 463-466, Albuquerque, N.M., June 1982.
16. R. H. Ott, R. G. Kouyoumjian, and Peters, "Scattering by a two dimensional periodic array of narrow plates", *Radio. Sci.*, vol. 2, pp. 1317-1349, Nov. 1967.
17. R. B. Keiburtz, and A. Ishimaru, "Scattering by a periodically apertured conducting screen", *IEEE Transactions on Antennas and Propagation*, vol. AP-3, pp. 506-544, Nov. 1961.
18. J. P. Montgomery, "Scattering by an infinite periodic array of thin conductors on a dielectric sheet", *IEEE Transactions on Antennas and Propagation*, vol. AP-23, pp. 70-75, Jan. 1975.
19. C. H. Tsao, R. Mittra, "A spectral-iteration approach for analyzing scattering from FSS's", *IEEE Transactions on Antennas and Propagation*, vol. AP-30, March 1982

APPENDIX A

FIELDS OF A PHASED LINE SOURCE

Consider a current filament located at $\rho = 0$, radiation into free space. The length of the filament extends to infinity and has a linear phase variation k_{z0} such that

$$\vec{I} = \bar{a}_z I_0 e^{-jk_{z0}z} \quad (\text{A-1})$$

where I_0 is a constant. The fields radiated can be represented in terms of a z-component of magnetic vector potential A_z since the electric current filament lies along z-axis [8]. That magnetic vector potential should satisfy the wave equation

$$\nabla^2 A_z + k_0^2 A_z = 0 \quad (\text{A-2})$$

After writing the operator ∇^2 in the cylindrical coordinated system and applying the separation of variable technique [8], we can obtain

$$A_z = [C_1 H_m^{(1)}(k_\rho \rho) + D_1 H_m^{(2)}(k_\rho \rho)] [C_2 \cos(m\phi) + D_2 \sin(m\phi)] [A_3 e^{-jk_z z} + B_3 e^{jk_z z}] \quad (\text{A-3})$$

where

$$k_\rho^2 + k_z^2 = k_0^2$$

is a dispersion relation for the problem. Also m is an integer. Note that since (A-1) has no ϕ variation A_z should have no ϕ variation as well. So we must choose

$m = 0$. In addition, we must choose Hankel function of the second kind to represent an outgoing wave. Thus

$$\begin{aligned} C_1 &= 0 \\ m &= 0 \\ A_z &= H_0^{(2)}(k_\rho \rho) [A_3 e^{-jk_z z} + B_3 e^{jk_z z}] \end{aligned} \quad (\text{A-4})$$

The remaining coefficients of A_z can be determined from the boundary condition

$$\lim_{\rho \rightarrow 0} \oint \vec{H} \bullet \vec{dl} = \lim_{\rho \rightarrow 0} \int H_\phi \rho d\phi = I_0 e^{-jk_{z0} z} \quad (\text{A-5})$$

which is known as the Ampere's Law. ϕ -component of magnetic field from (3.4.d) is

$$H_\phi = \frac{-1}{\mu_0} \frac{\partial}{\partial \rho} A_z = \frac{-1}{\mu_0} k_\rho H_0^{(2)}(k_\rho \rho) [A_3 e^{-jk_z z} + B_3 e^{jk_z z}] \quad (\text{A-6})$$

Now performing the integration of (A-5)

$$I_0 e^{-jk_{z0} z} = \frac{-1}{\mu_0} k_\rho [A_3 e^{-jk_z z} + B_3 e^{jk_z z}] \lim_{\rho \rightarrow 0} [\rho H_0^{(2)}(k_\rho \rho)] 2\pi \quad (\text{A-7})$$

and using small argument approximation to Hankel function

$$\lim_{\rho \rightarrow 0} \left\{ \rho H_0^{(2)}(k_\rho \rho) \right\} = \lim_{\rho \rightarrow 0} \left\{ \rho \frac{-j2}{\pi k_\rho \rho} \right\} = \frac{-j2}{\pi k_\rho} \quad (\text{A-8})$$

(A-7) becomes

$$I_0 e^{-jk_{z0} z} = \frac{j4}{\mu_0} [A_3 e^{-jk_z z} + B_3 e^{jk_z z}] \quad (\text{A-9})$$

In order for (A-9) to hold for all values of z , we can require

$$B_3 = 0 \quad (\text{A-10.a})$$

$$k_z = k_{z0} \quad (\text{A-10.b})$$

$$k_\rho^2 = k_{\rho 0}^2 = k_0^2 - k_{z0}^2 \quad (\text{A-10.c})$$

$$A_3 = \frac{I_0 \mu_0}{j4} \quad (\text{A-10.d})$$

Hence A_z becomes

$$A_z = \frac{\mu_0 I_0}{j4} H_0^{(2)}(k_{\rho 0} \rho) e^{-jk_{z0} z} \quad (\text{A-11})$$

Finally the radiated fields are, from equations (3.4),

$$E_z = \frac{-j}{\omega \mu_0 \epsilon_0} \left[\frac{\partial^2}{\partial z^2} + k_0^2 \right] A_z = \frac{-j [k_0^2 - k_{z0}^2] A_z}{\omega \mu_0 \epsilon_0} = - \left(\frac{k_{\rho 0}}{k_0} \right)^2 \frac{k_0 Z_0 I_0}{4} H_0^{(2)}(k_{\rho 0} \rho) e^{-jk_{z0} z} \quad (\text{A-12})$$

$$E_\rho = \frac{-j}{\omega \mu_0 \epsilon_0} \left[\frac{\partial^2}{\partial \rho \partial z} \right] A_z = \frac{jk_{\rho 0} k_{z0} Z_0 I_0}{4k_0} H_0^{(2)}(k_{\rho 0} \rho) e^{-jk_{z0} z} \quad (\text{A-13})$$

$$E_\phi = \frac{-j}{\omega \mu_0 \epsilon_0} \frac{1}{\rho} \left[\frac{\partial^2}{\partial \phi \partial z} \right] A_z = 0 \quad (\text{A-14})$$

$$H_z = 0 \quad (\text{A-15})$$

$$H_\rho = \frac{1}{\rho} \left[\frac{\partial}{\partial \phi} \right] A_z = 0 \quad (\text{A-16})$$

$$H_\phi = \frac{-1}{\mu_0} \left[\frac{\partial}{\partial \rho} \right] A_z = \frac{jk_{\rho 0} I_0}{4} H_0^{(2)}(k_{\rho 0} \rho) e^{-jk_{z0} z} \quad (\text{A-17})$$

The total complex power radiated from a length d of the current (A-1) can be found from the integral (see equation (4.41))

$$P = -\lim_{\rho \rightarrow 0} \left\{ \int_{-d/2}^{d/2} \int_0^{2\pi} E_z [I_0 e^{-jk_{z0} z}]^* d\phi dz \right\} \quad (\text{A-18})$$

If we use (A-12) in (A-18) and take the real part of P, we obtain the time average power radiated

$$P_{av} = \left(\frac{k_{\rho n}}{k_0}\right)^2 \frac{k_0 Z_0 I_0 I_0^*}{4} J_0(k_{\rho 0} 0) 2\pi d = \left(\frac{k_{\rho 0}}{k_0}\right)^2 \frac{k_0 Z_0 |I_0|^2}{4} 2\pi d \quad (\text{A-19})$$

Now if we divide (A-19) by the number of elements N and use $\alpha = 2\pi / N$, we find the time average power radiated into each unit cell

$$P_{cell} = \left(\frac{k_{\rho 0}}{k_0}\right)^2 \frac{k_0 Z_0 |I_0|^2 \alpha d}{4} \quad (\text{A-20})$$

It may be useful to notice that for a current filament of type (A-1), the radiated fields have no ϕ -variation as seen from the results. Therefore

$$\begin{aligned} v_0 &= 0 \\ v_m &= \frac{2\pi m}{\alpha} = mN, \quad m = 0, \pm 1, \pm 2, \dots \end{aligned} \quad (\text{A-21})$$

and the associated Floquet modes are

$$\psi_{mn} = \frac{e^{-j(v_m \phi + k_{zn} z)}}{\sqrt{\alpha d}} = \frac{e^{-j(mN\phi + (k_{z0} + 2\pi m/d)z)}}{\sqrt{\alpha d}} \quad (\text{A-22})$$

Specifically we can represent any field component derived in this appendix in terms of the fundamental mode ψ_{00} if we replace all $e^{-jk_{z0}z}$ factors by $\sqrt{\alpha d} \psi_{00}$. This type of representation of incident field simplified most of the integration operations of Chapter 4.

APPENDIX B

CONVERGENCE ACCELERATION FOR THE MATRIX ELEMENTS

In this appendix we describe a convergence acceleration method for the matrix elements A_{pq} given by (3.36) in Chapter 3, and (4.40) in Chapter 4

$$A_{pq} = \sum_{n=-\infty}^{\infty} \sum_{m=-\infty}^{\infty} \left(\frac{k_{\rho n}}{k_0} \right)^2 Z_{v_m} H_{v_m}^{(2)}(k_{\rho n} \rho_0) S_{v_m}^2 C_{nq}^* C_{np} \quad \text{in chapter 3 (B-1)}$$

$$A_{pq} = \sum_{n=-\infty}^{\infty} \sum_{m=-\infty}^{\infty} \left(\frac{k_{\rho n}}{k_0} \right)^2 J_{v_m}(k_{\rho n} a) H_{v_m}^{(2)}(k_{\rho n} a) S_{v_m}^2 C_{nq}^* C_{np} \quad \text{in chapter 3 (B-2)}$$

Here the coefficients are very similar for both (B-1) and (B-2), and we will present the convergence acceleration method only for (B-1) since it is a bit general. At the end of the chapter we will extend the result of this method to (B-2).

Recall from Chapter 3 that the coefficients of (B-1) are

$$Z_{v_m} = Z_{v_m}(k_{\rho n}; a, \rho_0) = \left[J_{v_m}(k_{\rho n} \rho_0) - \frac{H_{v_m}^{(2)}(k_{\rho n} \rho_0)}{H_{v_m}^{(2)}(k_{\rho n} a)} J_{v_m}(k_{\rho n} a) \right] \quad (\text{B-3})$$

$$S_{v_m}^2 = \frac{\sin^2[v_m x]}{[v_m x]^2}, \quad x = W/2\rho_0 \quad (\text{B-4})$$

$$C_{nq}^* = q \frac{[(-1)^q e^{jk_{zn}L/2} - e^{-jk_{zn}L/2}]}{(k_{zn}L)^2 - (q\pi)^2} \quad (\text{B-5})$$

$$C_{np} = p \frac{[(-1)^p e^{-ik_{zn}L/2} - e^{ik_{zn}L/2}]}{(k_{zn}L)^2 - (p\pi)^2} \quad (\text{B-6})$$

and

$$k_{\rho n}^2 = k_0^2 - k_{zn}^2, \quad v_m = v_0 + \frac{2\pi m}{\alpha} = v_0 + mN, \quad k_{zn} = k_{z0} + \frac{2\pi m}{d} \quad (\text{B-7})$$

$$m = 0, \pm 1, \pm 2, \dots; \quad n = 0, \pm 1, \pm 2, \dots$$

Since the coefficients C_{nq}^* , C_{np} , and $k_{\rho n}^2$ are independent from m , then we can write (B-1) in the form

$$A_{pq} = \sum_{n=-\infty}^{\infty} \left(\frac{k_{\rho n}}{k_0} \right)^2 C_{nq}^* C_{np} w_n \quad (\text{B-8})$$

where

$$w_n = \sum_{m=-\infty}^{\infty} f_{mn} \quad (\text{B-9})$$

and

$$f_{mn} = \frac{\sin^2(v_m x)}{(v_m x)^2} Z_{v_m} H_{v_m}^{(2)}(k_{\rho n} \rho_0) \quad (\text{B-10})$$

For convenience let $w_n = w_0 + w'_n$ where $w_0 = f_{0n}$ and

$$w'_n = \sum_{m=-\infty}^{\infty} ' f_{mn} \quad (\text{B-11})$$

The prime indicates the exclusion of the $m=0$ term in the infinite sum. To facilitate convergence acceleration of w'_n it is desirable to introduce the first-order large index asymptotic expression for $Z_{v_m} H_{v_m}^{(2)}$. To do this we can use the following asymptotic forms and identities from [7] for the Bessel functions with argument z and order ν

$$\lim_{\nu \rightarrow \infty} J_{\nu}(z) \approx \frac{1}{\sqrt{2\pi\nu}} \left(\frac{ez}{2\nu} \right)^{\nu} \quad (\text{B-12})$$

$$\lim_{\nu \rightarrow \infty} H_{\nu}^{(2)}(z) \approx j \sqrt{\frac{2}{\pi \nu}} \left(\frac{2\nu}{ez} \right)^{\nu} \quad (\text{B-13})$$

$$J_{-\nu}(z) = (-1)^{\nu} J_{\nu}(z) \quad , \quad H_{-\nu}^{(2)}(z) = (-1)^{\nu} H_{\nu}^{(2)}(z) \quad (\text{B-14})$$

Then it is obvious from (B-14) and (B-3) that

$$Z_{\nu_m}(k_{\rho m}; a, \rho_0) H_{\nu_m}^{(2)}(k_{\rho m} \rho_0) = Z_{|\nu_m|}(k_{\rho m}; a, \rho_0) H_{|\nu_m|}^{(2)}(k_{\rho m} \rho_0) \quad (\text{B-15})$$

and by using (B-12) and (B-13) we can write

$$\begin{aligned} & \lim_{m \rightarrow \infty} Z_{|\nu_m|}(k_{\rho m}; a, \rho_0) H_{|\nu_m|}^{(2)}(k_{\rho m} \rho_0) \\ & \approx \lim_{m \rightarrow \infty} \left[\frac{1}{\sqrt{2\pi|\nu_m|}} \left(\frac{ek_{\rho m} \rho_0}{2|\nu_m|} \right)^{|\nu_m|} - \frac{j \sqrt{\frac{2}{\pi|\nu_m|}} \left(\frac{2|\nu_m|}{ek_{\rho m} \rho_0} \right)^{|\nu_m|}}{j \sqrt{\frac{2}{\pi|\nu_m|}} \left(\frac{2|\nu_m|}{ek_{\rho m} a} \right)^{|\nu_m|}} \frac{1}{\sqrt{2\pi|\nu_m|}} \left(\frac{ek_{\rho m} a}{2|\nu_m|} \right)^{|\nu_m|} \right] j \sqrt{\frac{2}{\pi|\nu_m|}} \left(\frac{2|\nu_m|}{ek_{\rho m} \rho_0} \right)^{|\nu_m|} \\ & \approx \lim_{m \rightarrow \infty} \frac{j}{\pi|\nu_m|} \left[\left(\frac{ek_{\rho m} \rho_0}{2|\nu_m|} \right)^{|\nu_m|} - \left(\frac{a}{\rho_0} \right)^{|\nu_m|} \left(\frac{ek_{\rho m} a}{2|\nu_m|} \right)^{|\nu_m|} \right] \left(\frac{2|\nu_m|}{ek_{\rho m} \rho_0} \right)^{|\nu_m|} \end{aligned}$$

but since $\rho_0 > a$

$$\lim_{m \rightarrow \infty} Z_{\nu_m}(k_{\rho m}; a, \rho_0) H_{\nu_m}^{(2)}(k_{\rho m} \rho_0) \approx \lim_{m \rightarrow \infty} \frac{j}{\pi|\nu_m|} = \lim_{m \rightarrow \infty} \frac{j}{\pi|v_0 + mN|} = \frac{j}{\pi|m|N} \quad (\text{B-16})$$

This result also shows that the series (B-11) converges as $1/m$ which is very slow. In view of this result, we can rewrite (B-11) in the following useful form:

$$\begin{aligned} w'_n &= \sum_{m=-\infty}^{\infty} \left[\frac{\sin^2(v_m x)}{(v_m x)^2} Z_{\nu_m} H_{\nu_m}^{(2)}(k_{\rho m} \rho_0) - \frac{j \sin^2(v_m x)}{\pi |m|^3 N^3 x^2} \right] + \sum_{m=-\infty}^{\infty} \frac{j \sin^2(v_m x)}{\pi |m|^3 N^3 x^2} \\ &= \sum_{m=-\infty}^{\infty} \frac{\sin^2(v_m x)}{(v_m x)^2} \left[Z_{\nu_m} H_{\nu_m}^{(2)}(k_{\rho m} \rho_0) - \frac{j v_m^2}{\pi |m|^3 N^3} \right] + \frac{j}{\pi N^3 x^2} \sum_{m=-\infty}^{\infty} \frac{\sin^2(v_m x)}{|m|^3} \\ &= \sum_{m=-\infty}^{\infty} \frac{\sin^2(v_m x)}{(v_m x)^2} \left[Z_{\nu_m} H_{\nu_m}^{(2)}(k_{\rho m} \rho_0) - j \frac{v_0^2 + 2v_0 mN + m^2 N^2}{\pi |m|^3 N^3} \right] + \frac{j}{\pi N^3 x^2} \sum_{m=-\infty}^{\infty} \frac{\sin^2(v_m x)}{|m|^3} \\ &= \sum_{m=-\infty}^{\infty} \frac{\sin^2(v_m x)}{(v_m x)^2} \left[Z_{\nu_m} H_{\nu_m}^{(2)}(k_{\rho m} \rho_0) - j \frac{1}{\pi |m| N} - j \frac{v_0^2 + 2v_0 mN}{\pi |m|^3 N^3} \right] + S \end{aligned} \quad (\text{B-17})$$

where

$$\begin{aligned}
S &= j \frac{1}{\pi N^3 x^2} \sum_{m=-\infty}^{\infty} \frac{\sin^2(v_m x)}{|m|^3} = j \frac{1}{\pi N^3 x^2} \sum_{m=-\infty}^{\infty} \frac{1 - \cos(2v_m x)}{2|m|^3} \\
&= j \frac{1}{2\pi N^3 x^2} \sum_{m=-\infty}^{\infty} \frac{1}{|m|^3} - j \operatorname{Re} \left\{ \frac{1}{\pi N^3 x^2} \sum_{m=-\infty}^{\infty} \frac{e^{j2v_m x}}{2|m|^3} \right\} \\
&= j \frac{1}{\pi N^3 x^2} \sum_{m=1}^{\infty} \frac{1}{m^3} - \frac{j}{\pi N^3 x^2} \operatorname{Re} \left\{ e^{j2v_0 x} \sum_{m=-\infty}^{\infty} \frac{e^{j2mNx}}{2|m|^3} \right\} \\
&= j \frac{1}{\pi N^3 x^2} \sum_{m=1}^{\infty} \frac{1}{m^3} - \frac{j}{\pi N^3 x^2} \operatorname{Re} \left\{ e^{j2v_0 x} \sum_{m=1}^{\infty} \frac{2 \cos(2mNx)}{2|m|^3} \right\} \\
&= j \frac{1}{\pi N^3 x^2} \sum_{m=1}^{\infty} \frac{1}{m^3} - \frac{j}{\pi N^3 x^2} \cos(2v_0 x) \sum_{m=1}^{\infty} \frac{\cos(2mNx)}{|m|^3} \\
&= \frac{j}{\pi N^3 x^2} [E - \cos(2v_0 x) F(x)]
\end{aligned} \tag{B-18}$$

A computer program may be used to evaluate E

$$E = \sum_{m=1}^{\infty} \frac{1}{m^3} = 1.2020569031... \tag{B-19}$$

and

$$F(x) = \sum_{m=1}^{\infty} \frac{\cos(2mNx)}{|m|^3} \tag{B-20}$$

Now, one observes that the series in (B-17) converges now as $1/m^2$. The sum $F(x)$ in (B-20) may be evaluated with the aid of a rapidly convergent series given in [4]

$$F(x) = 1.2020569031 + (Nx)^2 \left[2 \ln(2Nx) - 3 - \frac{(Nx)^2}{18} - \dots \right] \tag{B-21}$$

Hence the matrix elements A_{pq} become

$$\begin{aligned}
A_{pq} &= \sum_{n=-\infty}^{\infty} \left(\frac{k_{\rho n}}{k_0} \right)^2 C_{nq}^* C_{np} (w_0 + w'_n) \\
&= \sum_{n=-\infty}^{\infty} \left(\frac{k_{\rho n}}{k_0} \right)^2 C_{nq}^* C_{np} \left\{ S_{v_0}^2 \left[Z_{v_0} H_{v_0}^{(2)}(k_{\rho n} \rho_0) \right] + S \right. \\
&\quad \left. + \sum_{m=-\infty}^{\infty} S_{v_m}^2 \left[Z_{v_m} H_{v_m}^{(2)}(k_{\rho n} \rho_0) - j \frac{1}{\pi |m| N} - j \frac{v_0^2 + 2v_0 m N}{\pi |m|^3 N^3} \right] \right\}
\end{aligned} \tag{B-22}$$

The result (B-22) can also be used for the matrix elements (B-2) after a modification. It can be shown by using (B-12), (B-13), and (B-14) that the asymptotic form of the product of Bessel functions in (B-2) is

$$\lim_{m \rightarrow \infty} J_{v_m}(k_{\rho m} a) H_{v_m}^{(2)}(k_{\rho m} a) \approx \frac{j}{\pi |m| N} \tag{B-23}$$

which is the same of the result obtained in (B-16). Hence, by introducing (B-23) in to (B-2) one can obtain

$$\begin{aligned}
A_{pq} &= \sum_{n=-\infty}^{\infty} \left(\frac{k_{\rho n}}{k_0} \right)^2 C_{nq}^* C_{np} (w_0 + w'_n) \\
&= \sum_{n=-\infty}^{\infty} \left(\frac{k_{\rho n}}{k_0} \right)^2 C_{nq}^* C_{np} \left\{ S_{v_0}^2 \left[J_{v_0}(k_{\rho n} a) H_{v_0}^{(2)}(k_{\rho n} a) \right] + S \right. \\
&\quad \left. + \sum_{m=-\infty}^{\infty} S_{v_m}^2 \left[J_{v_m}(k_{\rho n} a) H_{v_m}^{(2)}(k_{\rho n} a) - j \frac{1}{\pi |m| N} - j \frac{v_0^2 + 2v_0 m N}{\pi |m|^3 N^3} \right] \right\}
\end{aligned} \tag{B-24}$$

Here S is given by (B-18), (B-19), and (B-20) but $x = W / 2a$ for this case.